ingegneria sismica
International Journal of Earthquake Engineering
Anno XXXVIII – Num.4 - 2021

SEISMIC VULNERABILITY ASSESSMENT OF EXISTING RC STRUCTURES SUBJECTED TO MULTIPLE EARTHQUAKES.

Kainaat Nadeem[1], Aslam Faqeer Mohammad[2]

[1, 2] Department of Civil Engineering, NED University of Engineering and Technology, Karachi, Pakistan

SUMMARY: *Multiple earthquakes occur all over the world where challenging fault systems exist. A structure damaged by an earthquake is exposed to the risk of aftershocks within a short interval of time, which accumulates damage to the structure affecting its stiffness, strength and ductility. This study aims to investigate the response of reinforced concrete infilled frames subjected to multiple ground motion sequences. A two dimensional computational model of a mixed used RC building located in Karachi, Pakistan is developed as a bare and infilled frames for comprehensive comparative analyses. Initially, nonlinear static pushover analysis was used to estimate the capacities and damage patterns of frames. Finally, to track the complete response selected frames were subjected to three real seismic sequences (recorded at a short interval of time at same station with same direction) and four artificially generated repeated seismic sequences. Results are presented in the form of Engineering Demand Parameters (EDPs), which conforms the effects of multiple earthquakes particularly in the case of infilled frame.*

KEYWORDS: *Multiple Earthquakes, Nonlinear Pushover Analysis, Response History Analysis, Infilled frame, Residual Displacement, Residual Drift*

1 Introduction

Pakistan is considered to be a seismically active region due to its seismotectonic settings. The seismotectonic settings of Pakistan creates a push in Northern part forming Himalyas and a subduction zone in southern part of the country making it one of most seismically active region in the world [Waseem *et. al.*, 2019]. Karachi is located directly on a triple junction point of the Arabian, Indian and Asian plates, which exposes it to a high seismic risk (figure-01). Although there is limited historical documentation for any earthquakes experienced by this city, but it has felt damaging vibrations in the past nearly 200 years ago due to active structural zones[Bilham *et al.*, 2007]. According to Pakistan's most recent seismic zoning map, Karachi lies in Zone 2B which makes it close to experience a devastating earthquake in the coming years although no documentation exists to prove that it has been hit by any seismic activity in the past, which could be due to unreliable historical data.

Corresponding author: Kainaat Nadeem, Department of Civil Engineering, NED University of Engineering and Technology, Pakistan.
Email: kainaat@neduet.edu.pk

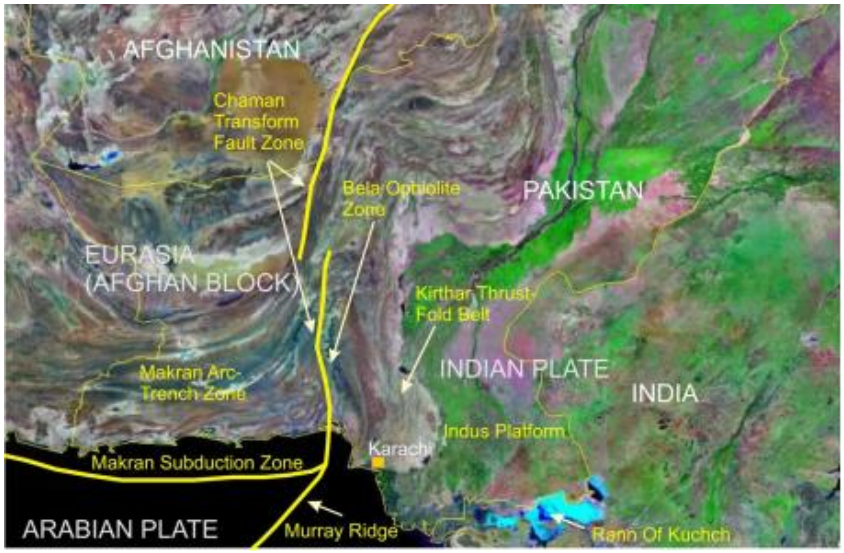

Figure 1 *Seismotectonic settings of Karachi in reference with the plate boundaries and tectonics zones of southern Pakistan* [Waseem *et. al.*, 2019].

(a) (b)

(c)

Figure 2 *Existing infilled frame structures in Karachi, (a) Multistory hospital building under renovation, (b) Arts council building and (c) Typical mid-rise residential apartment building.*

Non-engineered reinforced concrete infilled frame is a typical existing building typology in Karachi that is vulnerable to significant damage in moderate to severe earthquakes. Figure 2 depicts some of Karachi's existing reinforced concrete infilled framed structures. The seismic code documented in Pakistan is adopted by UBC 97 [UBC-1997, 1997], which provides a false representation for the majority of structures designed in Pakistan because detailing and design practices are not done in accordance with the adopted building code, resulting in inadequate and incompetent building and loss of life if a calamity strikes. This has been experienced in the past two years when a number of multi-story buildings collapsed in Karachi (figure 3), prompting the government to declare four hundred buildings in the city decrepit and 1,500 dangerous, but they could not be evacuated. It is pertinent to mention that 17 people, including women and children, were killed in an accident in Rizvia Society, Karachi where a residential building collapsed. Following the December 2019 demolition of a six-story building in Karachi's Timber Market area, three people were killed and three others were injured when a building collapsed in Malir Jafar Tayar Society in February 2019. Six people were killed and dozens were injured in July 2017 when a three-story building in the Liaquatabad-No 9 area collapsed (The News International, September 2020). As a result, the recent calamities have added fuel to the underlying danger that Karachi will face if indigenous solutions are not provided.

The philosophy behind earthquake resistant design is that a building should be able to resist a ground motion without collapsing, but some damage is acceptable. As a result, the seismic loads imposed on the structure are far greater than its design capacity. When such structures are subjected to multiple earthquakes they fail under repetitive shaking due to accumulation of damage.

The performance-based earthquake engineering (PBEE) model can forecast both direct and indirect infrastructures losses caused by earthquakes. However, aftershocks from earthquakes, which can cause additional damage to structures, are still not taken into account in current techniques. The various post-quake decisions, such as evacuation and facility repair, are explicitly dependent on the performance assessment in light of the aftershocks.

Sequential tectonic activities, as observed in previous seismic event, generally accelerate the cumulative damage in structures, particularly in RC building structures. The earthquake in Christ Church had a magnitude of 7.1 Richter and was followed by an earthquake with a magnitude of 6.2 Richter, resulting in an increase in the number of collapsed structures. Similarly, a 5.7 Richter magnitude earthquake struck Turkey a few weeks after a 7.2 Richter magnitude earthquake, increasing the number of severely damaged and completely collapsed buildings. As a result, it is necessary to investigate the response of existing RC infilled frame structures to multiple shocks.

More often research was carried on the vulnerability assessment of structures under the most damaging earthquake, but the effects of prior shaking were neglected by estimating the loss of structure's lateral force resisting capacity [Hanson, 1996].

A very limited literature is available on the investigation of multiple earthquake effects. Because of their simplicity in implementing a degrading hysteretic relation, SDOF systems were previously used to study multiple earthquake responses. [Mahin, 1980] used the Managua earthquake (1972) as the main shock and two subsequent great aftershocks to present a cumulative ductility spectra that stated that the main shock caused a significant deformation to the initial strength of structure, whereas the second after shock caused a significant inelastic deformation and enhanced the ductility and energy dissipating demands of structure.

Figure 3 *Building collapse in Karachi*

He concluded that aftershock had no significant impact on the displacement and damage to the SDOF system with a note for further investigation. Amadio [Amadio et al., 2003] utilized three different hysteretic models to investigate the nonlinear behavior of SDOF structures using multiple excitations: non-degrading stiffness and strength, degrading stiffness and non-degrading strength, degrading stiffness and strength. They concluded that elastoplastic systems are the most vulnerable SDOF systems, but this study only included three ground motion sequences. Hatzigeorgiou, George and Beskos [Hatzigeorgiou et al., 2009] and -(George et al., 2010)] executed an exhaustive parametric analysis to study the effect of multiple earthquakes on a number of SDOF systems, concluding that sequential ground motions lead to increased displacement demands and affect the inelastic displacement ratios. Because these works are for SDOF systems and do not represent framed structure, component level degrading models were developed to study the behaviour of moment resisting frames.

Li and Elingwood [Li et al., 2007] measured the performance of steel moment resisting frames with moment-rotation joints that experienced connection fractures during the main and subsequent aftershock. The enhanced uncoupled modal response history analyses (EUMRHA) which is a modification of a method developed by Chopra and Goel [Chopra and Goel, 2001] was adapted for stochastic analyses of frames. This study concluded that emulating the main-aftershock assumption did not result in significant aftershock damage because damage was dependent on the amplitude and frequency of the aftershock ground motion.

Hatzigeorgiou and Liolios [Hatzigeorgiou et al., 2010] investigated the effectiveness of component-level-based models under multiple excitations, assuming bilinear moment-rotation relationships at beam-column connections. The researchers came to the conclusion that residual displacements have a major impact on stiffness deterioration.

Gracia [García, 2012] investigated the structure's displacement response under both synthetic and real seismic sequences using a randomized, back-to-back technique. They came to the conclusion that, when compared to documented earthquake sequences, simulated seismic sequences could lead to an overestimation of peak and residual drift needs. However, when aftershock is taken into account, their lateral drift requirements would grow. Furthermore, an assessment of real seismic sequences revealed that the primary shock and aftershock frequency content were only marginally associated.

This back-to-back technique ignored the differences between the primary shock and aftershock sequences, but it does reflect the aftershock reaction and cumulative damage status to some extent.

The influence of stiffness and strength degradation on reinforced concrete structures after recurrent earthquakes was studied by Abdelnaby and Elnashai[Abdelnaby et al., 2012]. Plastic energy damage concrete { Lee and Fenves, 1998][Lee and Fenves, 1998] and a modified Magnetto Pinto Steel model [Gomes and Appleton, 1997] were used to incorporate numerical models for SDOF and MDOF systems. Two real ground motion sequences, Christchurch and Loma Preita, were used with a time gap of 10 to 20 seconds between them. When compared to initially undamaged constructions, damaged frames (under repeated loading) attracted less seismic forces and performed better, underlining the need to further examine the effect of multiple ground motion shaking on a structure.

Oyguc [(Oyguc et al., 2018)] determined the effect of degrading behavior in irregular reinforced concrete buildings subjected to Tohoko and 23 artificial ground motion sequences using Plastic damage model by [Lee and Fenves, 1998] and a modified Magnetto Pinto Steel model [Gomes and Appleton, 1997] previously implemented by [Abdelnaby and Elnashai, 2014]. A comparative study was performed between the regular and irregularly framed buildings using SPEAR, ICONS and a school building located in the vicinity of Van, Turkey. This study concluded that irregular structures attract a significant amount of damage than their regular counterparts for Tohoko earthquake sequence.

The influence of repeated seven (07) seismic shocks on the inelastic response of reinforced concrete infilled frames has been examined in the current study. The first three seismic sequences were recorded at the same location, in the same direction, and at a short time interval. The remaining four seismic sequences are synthesized by applying a single ground motion to a back-to-back, repeating approach. Using the finite element programme ETABS[CSI, 2016], a mixed-use residential building is idealized as a two-dimensional frame (bare and infilled frames) and evaluated for nonlinear static and reaction history studies. The results are then compared to bare and infilled frame models that have been subjected to several earthquake episodes. The distribution of plastic hinges or damage patterns, as well as residual and maximum displacements, residual and transient inter-story drift ratios, and residual and transient inter-story drift ratios, are all analyzed in order to draw conclusions.

2 Description of Building Model

Figure 4 depicts a ground plus five stories mixed use apartment building in Gulistan-e-Johar, Karachi, Pakistan [NED and GHI, 2012]. The ground floor is for commercial use, while the above floors are earmarked for exclusive residential flats. The ground floor is reserved for commercial purpose and the floors above are exclusive residential apartments. The exterior dimension of building is 96 feet (28.8 m) wide and 72 feet (21.6 m) long and the height of building is 72 feet (21.6 m) tall approximately with a typical height of 12 feet (3.6 m) for all stories. The structural system of the building consists of reinforced concrete moment resisting frames with unreinforced block masonry infill walls and an eccentrically located reinforced concrete core. The blocks of infill walls are 6 inch (15 cm) thick. The foundations laid out are reinforced concrete spread footings. Majority of the residential building located in Pakistan are similar to the building studied herein. To track the interaction of infill panel with frame components, identified structure is analyzed for bare and infilled frames separately.

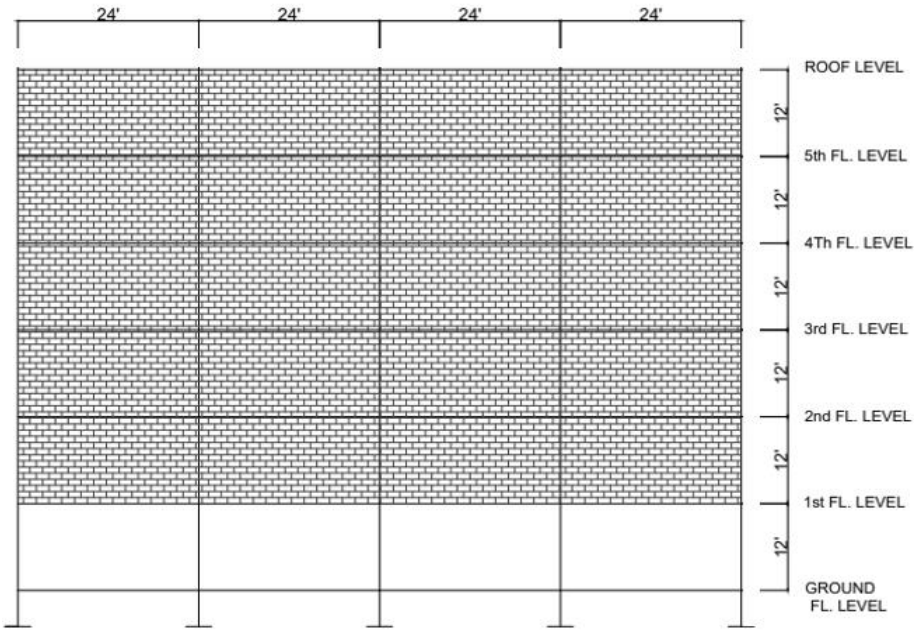

Figure 4 *Structural elevation of the building* [NED and GHI, 2012]

2.1 Computational model: Bare frame

The building is modeled is a four bay frame and the distance between each column is 24 feet (7.2 m). The beam size was taken as 12 in (30 cm) by 24 in (60 cm) and column size was 18 in (45 cm) by 18 in (45 cm) throughout the height of building. A 2% and 4% area of steel was considered for exterior and interior columns from base to second floor respectively and 1% and 2% area of steel was considered for exterior and interior columns up to the roof respectively. The thickness of slab was assumed to be 6 in (15 cm). The concrete compressive stress $f'c$ and the yield strength of steel fy were taken as 3000 psi (20.6 MPa) and 60000 psi (414 MPa) respectively. Figure 5 shows the section properties and detail of reinforcement for beams and columns. The building is evaluated for gravity and lateral loads. The gravity loads were uniformly distributed over the beams and the lateral loads were considered to be inverted triangular distributions. The addition of a floor slab increases the reinforced concrete structure's overall lateral rigidity (Montuori R. et al, 2016). According to published literature, slab elements play a substantial role in the seismic response of reinforced concrete structures (Montuori R. et al, 2021). The presence of floor joists in RC building, can have a significant impact on the structural response to lateral loads (Montuori R. et al, 2019). In general, slab elements are ignored in nonlinear time history analysis because they are computationally expensive. Similar to conventional practice, in current study for simplicity in nonlinear time history analyses, presence of slab on beam elements is taken into account by incorporating rigid diaphragm effects. Also, to capture the true seismic weight of entire structure, the self-weight corresponding to the tributary width of slab and superimposed dead loads such as floor finishes and masonry loads are also applied on the beam elements. This simplification increases the flexibility of the structure and overestimate the chord rotations in beam-column elements which needs to be further investigated in future research. Since the building is a regular residential building so the performance criteria of life safety was selected to evaluate the building response. Table 1 summarizes the list of loads applied on the frame.

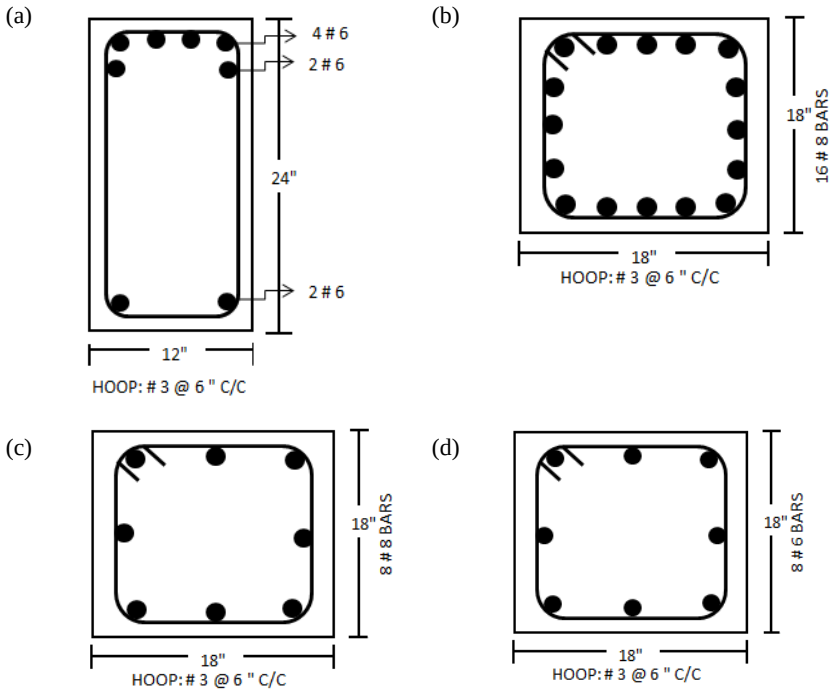

Figure 5 *Structural detail of (a) Typical beam, (b) Interior column from base to 2nd floor, (c) (c) Exterior column from base to 2nd floor, Interior column from 3rd to roof and (d) Exterior column from 3rd to roof*

Table 1 *Summary of loads applied on the two dimensional frame*

Applied load on Frame
– **Dead Load:**
– 1)Self weight of frame member
– 2) 6 inches (15 cm) thick slab
– 3) 2 inches (5 cm) thick finishes
– 3)Wall Load=50 psf (2.4 KPa)
– **Live Load:**
– 1) Floor: 50 psf (2.4 KPa)
– 2) Roof: 30 psf (1.5 KPa)

2.2 Computational model: Infilled Frame

A detailed literature review was done on the influence and modeling strategies of masonry infill which concluded that a macro modelling approach would be followed. In the current study the width of the compression strut was determined using Mainstone and Week's equation (Mainstone, 1971) which has been adopted by FEMA 356. The expression for equivalent strut width used is as follows:

$$w = 0.175\, d_{inf}\left(\lambda_{inf} H_{inf}\right)^{-0.4} \quad (1)$$

The compression struts were computed using the lower bound approach for masonry properties in [FEMA356, 2000], the compressive strength of masonry infill was 300 psi (2.07 MPa) and the width of diagonal strut was computed to be 35 inches (88 cm) using equation 1. No

alteration was made in structural detailing and properties of bare frames and modelled infills were added from 2nd story onwards. Figure 6 shows the idealized two dimensional bare and infilled frames modeled in ETABS to carry out nonlinear static and response history analyses.

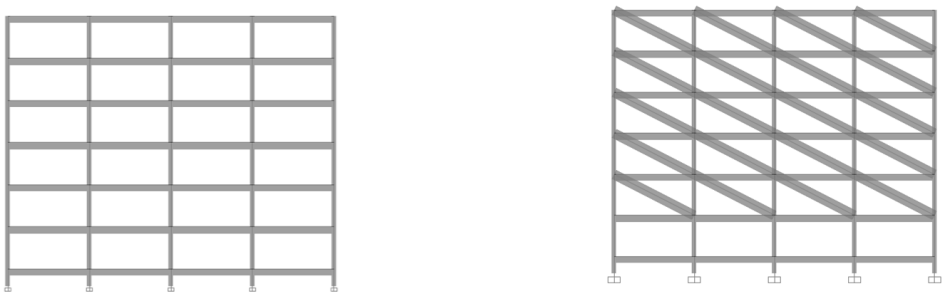

(a) (b)

Figure 6 *Idealized two dimensional (2D) frame computational model on ETABS (a) without infill and (b) with infill walls.*

3 Strut Inelasticity in Model

There are numerous state-of-the-art techniques available to capture the response of infill-frame interactions, these techniques are categorized as Micro-modeling, Meso-modeling and Macro-modeling. In current study, material nonlinearity is considered using macro modeling approach by modelling beam, column and compression struts as elastic elements and plastic hinges are defined at both ends of beams and columns and in the middle of compression struts.

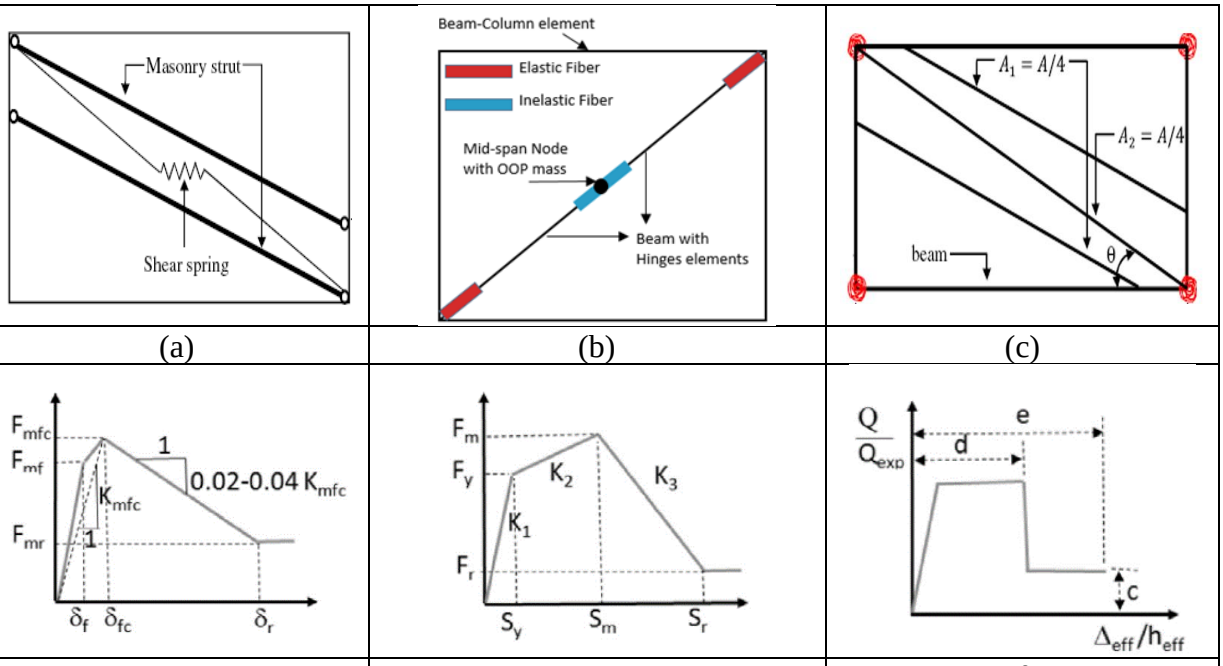

(a) (b) (c)

(d) (e) (f)

Figure 7 *(a) Crisafulli 1997, (b) Mosalam et al. 2009, (c) El-Dakhakhni 2003, (d) Bertoldi et al. 1993, (e) Fardis & Panagiotakos 1997, and (f) FEMA 356 model.*

This approach is employed since it is easy to incorporate in low to midrise framed structures and requires less computational efforts particularly in nonlinear dynamic analyses. As stated earlier several state-of-the-art models reported in literature few are shown in Figure 7.
Amongst these state-of-the-art models in the current study, FEMA356 model [FEMA356, 2000] force-displacement rule was adopted to model the plastic hinge properties of frame elements and compression struts as shown in Figure 7.A sectional analysis for beams and columns was done first by using the software Response 2000 [Bentz and Collins, 2000] to get moment-rotation curves. Figure 8 shows the Rotation and displacement control parameters for nonlinear hinges of beams, columns and compression struts.

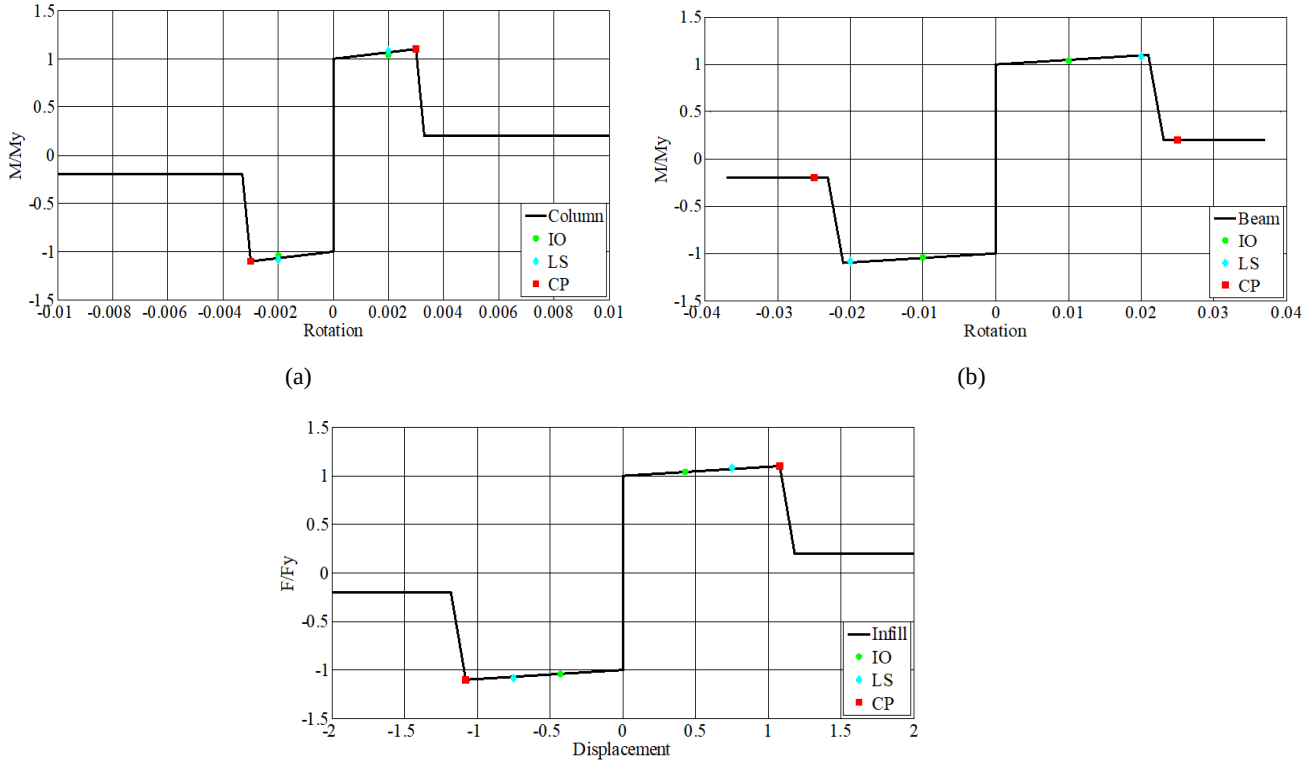

Figure 8 *Displacement control parameters for nonlinear hinges (a) beam (b) column and (c) Infill strut.*

4 Seismic Input

There are no ground motion records available for Karachi as there is still uncertainty about the seismic risk of this region therefore for performing multiple earthquake analysis on the building frame systems a suit of ground motions is selected randomly.
Figure 9 illustrates the contours of estimated PGA values for a return period of 475 and 2500 years [Ahmed *et al.*, 2019]. The return period of 475 and 2500 years corresponds to life safety and collapse prevention performance indicator respectively. According to the building code of Pakistan [MoHW, 2007] PGA for a return period of 2500 years is used for designing Dams but due to uncertainty associated with seismic hazard in Karachi reported by different authors [Bilham *et al.*, 2007, Waseem *et al.*, 2019 and Ahmed *et al.*, 2019]. In the current study, the infilled and their bare counterparts are analyzed through the suite of ground motions scaled on

peak ground acceleration corresponding to 2500 years return period with 2% probability of exceedance.

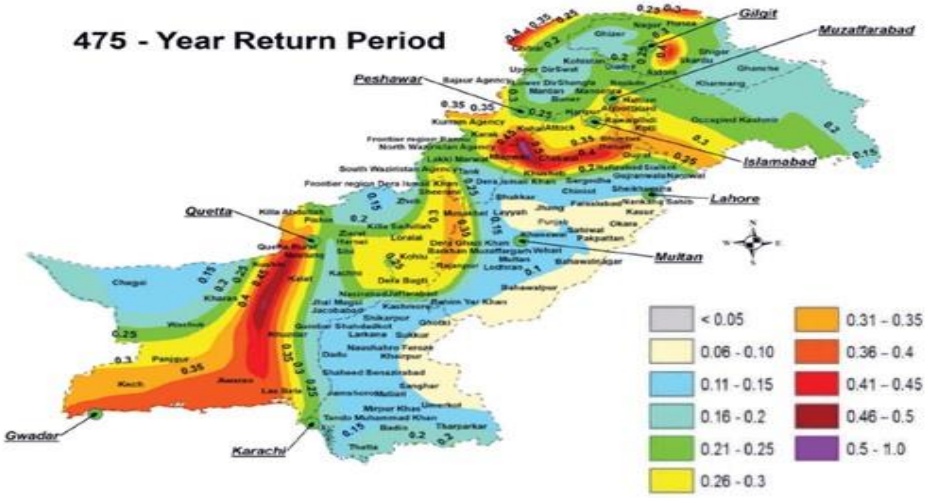

(a)

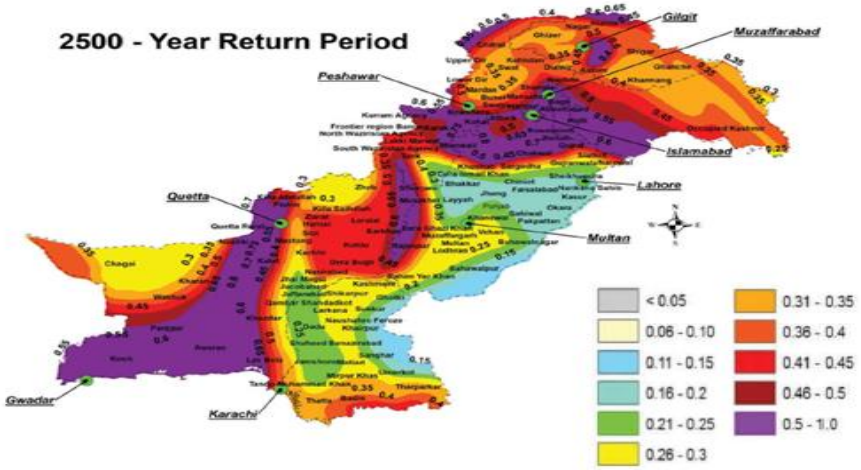

(b)

Figure 9 *Peak ground acceleration map for return period of (a) 475 years and (b) 2500 years* [Ahmed *et al.*, 2019].

4.1 Real seismic sequence

The first strong ground motion database consists of three real seismic sequences which are recorded during a short period of time (up to three days), at the same station, same direction and at same fault distance. These real sequences are Coalinga, Whittier Narrows and Imperial Valley earthquakes. Table 2 shows the parameters for these real sequences which were extracted from the strong motion database of the Pacific Earthquake Engineering Research (PEER) Center [PEER Center., 2017]. These ground motions were scaled using a spectral matching technique in time domain by employing the target spectrum obtained from ASCE 7-10 corresponding to maximum considered earthquake (MCE). A time buffer of 100 seconds is applied between the successive ground motion records as shown in Figure 10. The elastic spectra for this database with viscous damping ratio $\xi = 5\%$ are presented in Figure 11.

Table 2 *Seismic parameters of real sequential ground motion.*

Real Seismic Sequence			
Ground Motion	**Station**	**Date & Time**	**PGA(g)**
Coalinga	14th & Elm (Old Chap)	1983/7/22	0.42
		1983/7/25	0.47
Whittier Narrows	San Marino- SW Academy	1987/10/01	0.13
		1983/10/04	0.15
Imperial Valley	5055 Holtville P.O.	1979/10/15 (23:16)	0.26
		1979/10/15 (23:19)	0.12

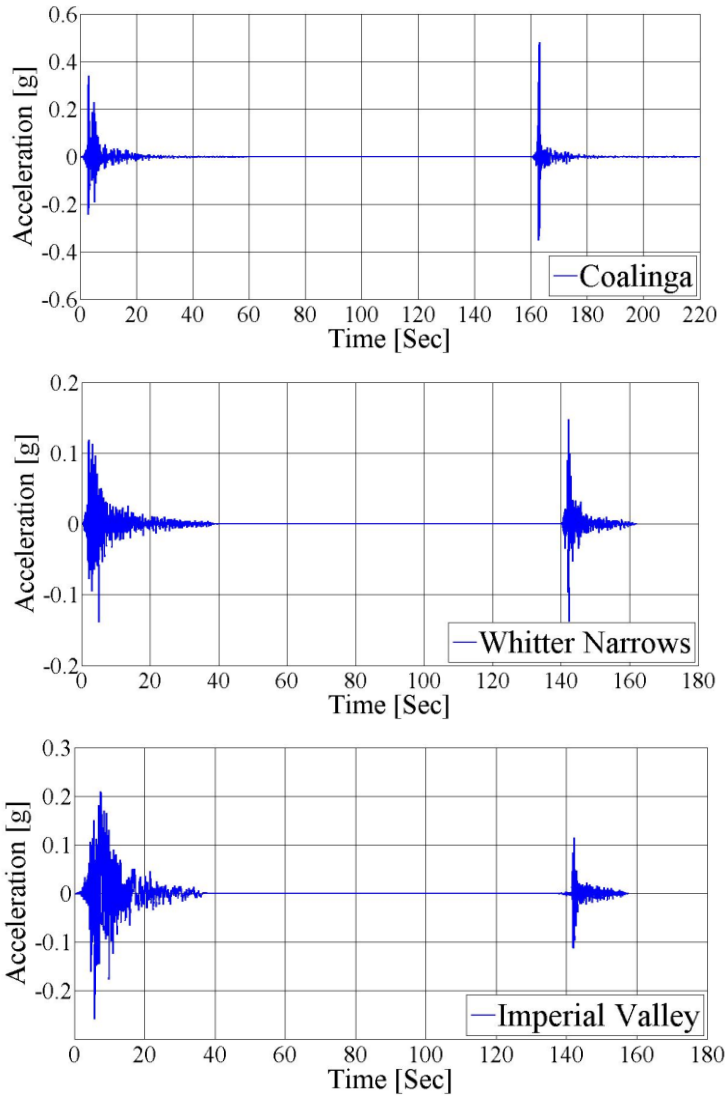

Figure 10 *Acceleration time history records of three real seismic sequences.*

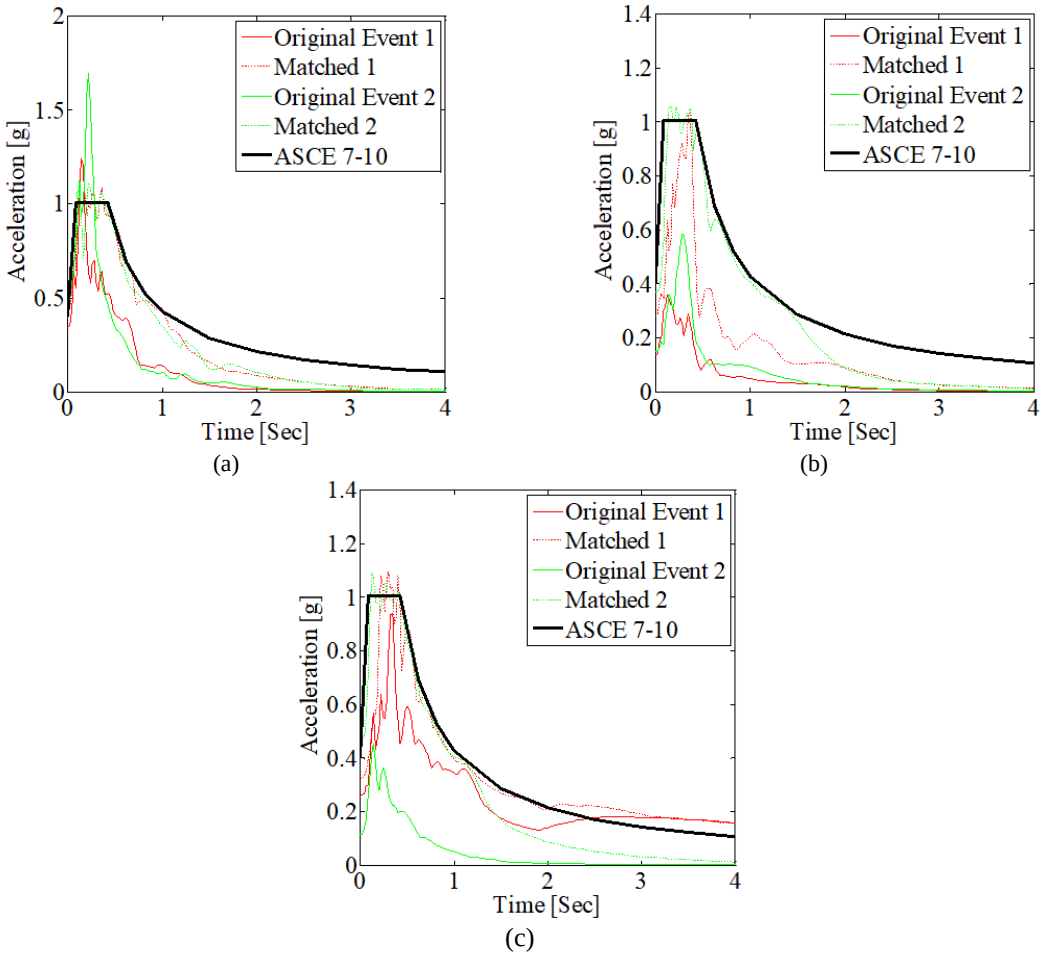

Figure 11 *Elastic response spectra of (a) Coalinga, (b) Whittier Narrows, and (c) Imperial Valley ground motions.*

4.2 Artificial seismic sequence

The second strong ground motion database consists of four artificial seismic sequences, more specifically two identical ground motions are applied in series creating a synthetic sequence which is due to the back-to-back repeated approach. Since spectral matching technique in time domain was used to scale the ground motions. Table 3 shows the parameters for single ground motions which were used to create a synthetic seismic sequence. A time buffer of 100 seconds is applied between the successive ground motion records as shown in Figure 12. The elastic spectra for this database with viscous damping ratio $\xi = 5\%$ are presented in Figure 13.

Table 3 *Seismic Parameters of Artificial ground motions.*

Ground Motion	**Station**	**PGA(g)**
Altadena	Eaton Canyon Park	0.44
Corralitos	Eureka Canyon Road	0.63
Santa Monica	City Hall	0.37
Hollister	South Street and Pine	0.37

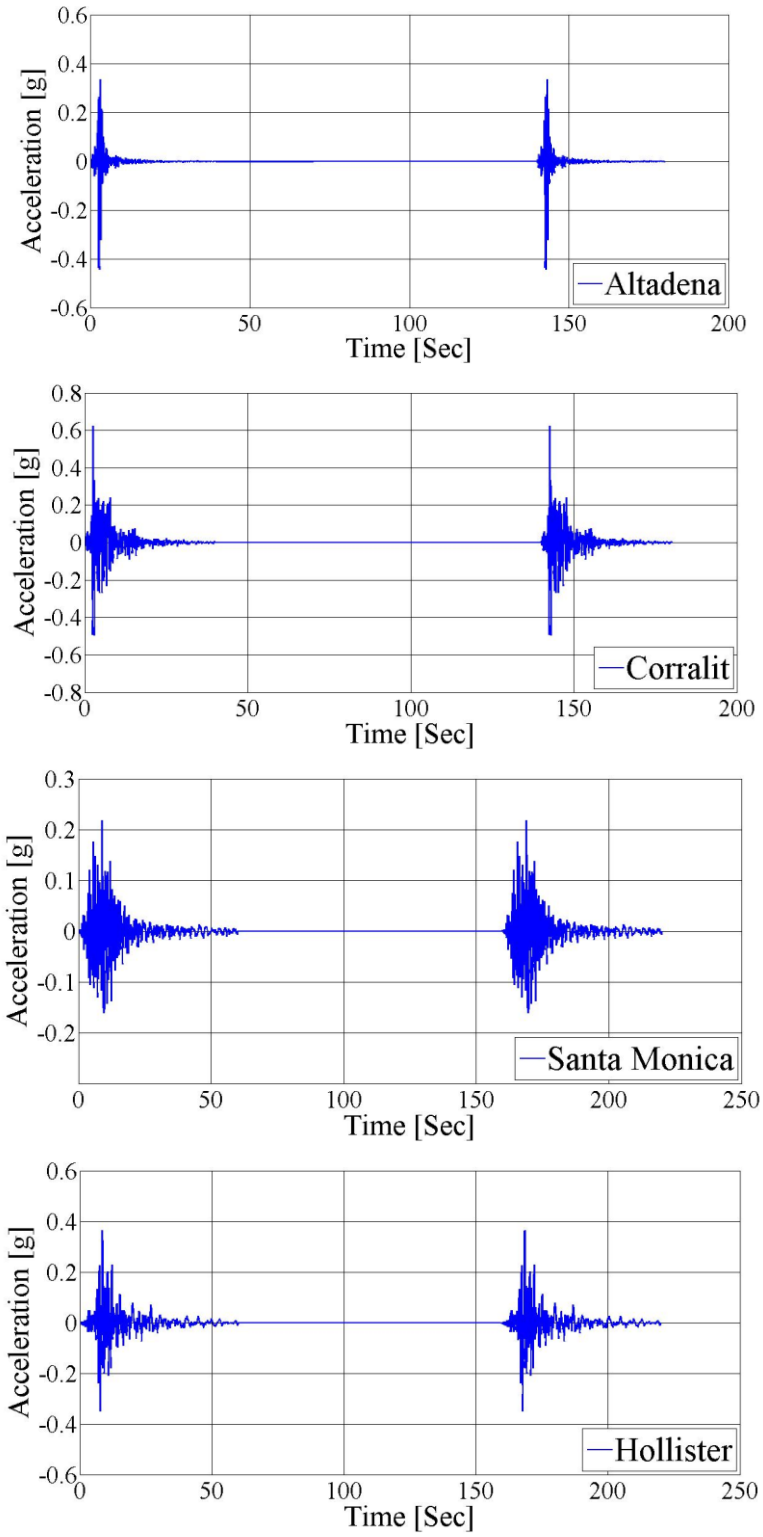

Figure 12 *Acceleration time history record of artificial seismic sequences*

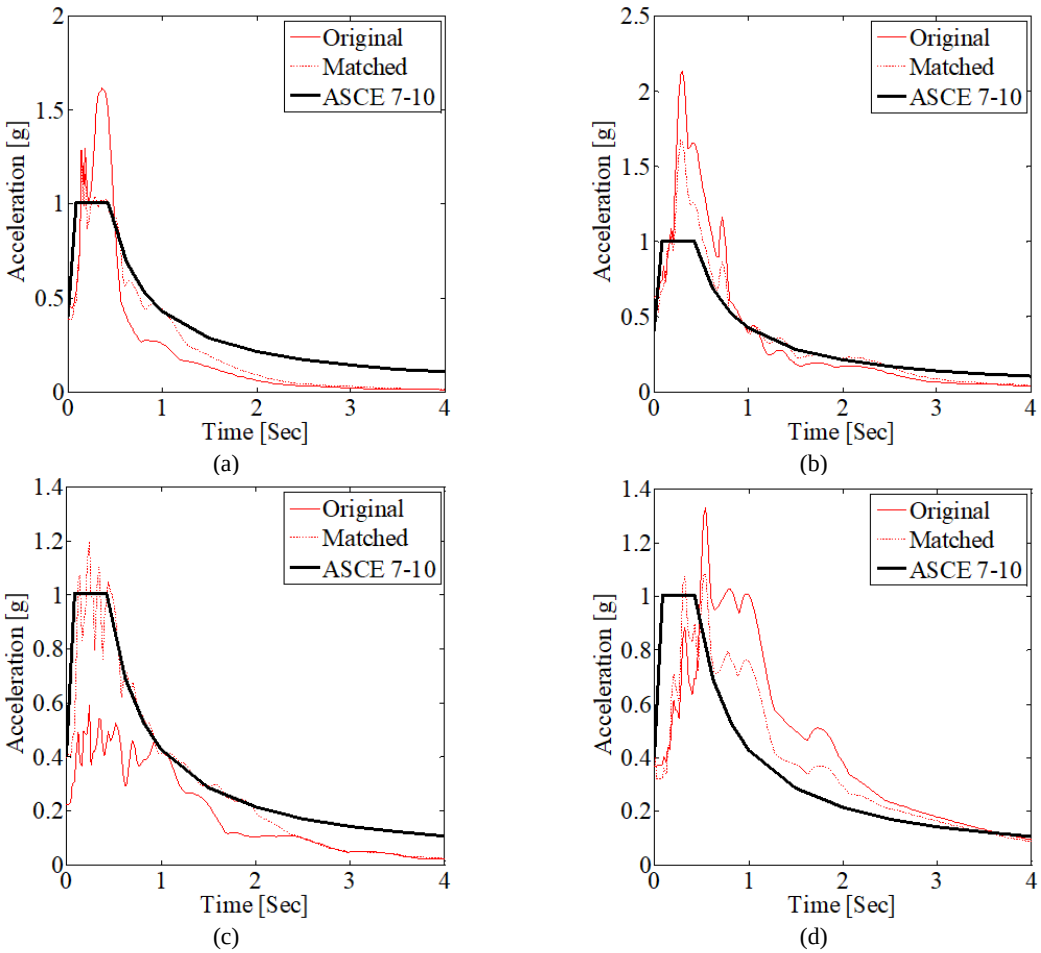

Figure 13 *Elastic response spectra of (a) Altadena, (b) Corralit, (c) Santa Monica, and (d) Hollister ground motions.*

5 Analysis and results

5.1 Nonlinear static pushover analyses for bare and infilled frames

Nonlinear static pushover (NSP) analysis is a procedure which determines the capacity of the structure in the form of a simple plot between the base shear and displacement of the structure. Inelastic static procedures require simple model representations and less number of analyses when compared with dynamic analyses[Mwafy and Elnashai, 2014].

Conventional pushover analyses are adopted for conducting on the frames for determining the real capacity of the bare and infill and their performance level. The localized failure in beam and columns are monitored by observing the formation of plastic hinges and soft story in bare and infill frames.

Before applying the pushover load, the frames are subjected to constant gravity loads using the combination *1.0 D.L + 0.25 L.L* as per code [ASCE 41-17, 2017] .

Where D.L is dead loads of the structure including self-weight of beam, columns, slabs, walls and super imposed loads and L.L is live load applied on the structure. Then the structure is

subjected to incrementally increasing monotonic loads in triangular pattern in X-Direction of the frames.

Figure 14 shows the capacity curves of the bare and infilled frames in the form of a plot between roof drifts and normalized base shear. A performance point is found with the intersection of capacity and demand spectra for both the frames using ASCE 41-17 NSP (Nonlinear Static Pushover) method. The graphs show that capacity of an infilled frame is much greater than its bare counterpart since infills increases the stiffness of structure and attracts more seismic forces. Figure 14 also shows the distribution of plastic hinges in bare and infilled frames. A unique color identity was given to each limit state, green for Immediate occupancy, cyan for Life Safety and red for Collapse prevention. Figure 12 shows the damage at performance point and observed significant damage in an infilled frame since the columns above the plinth level yields to a Life Safety limit state criteria as compared to the bare frame.

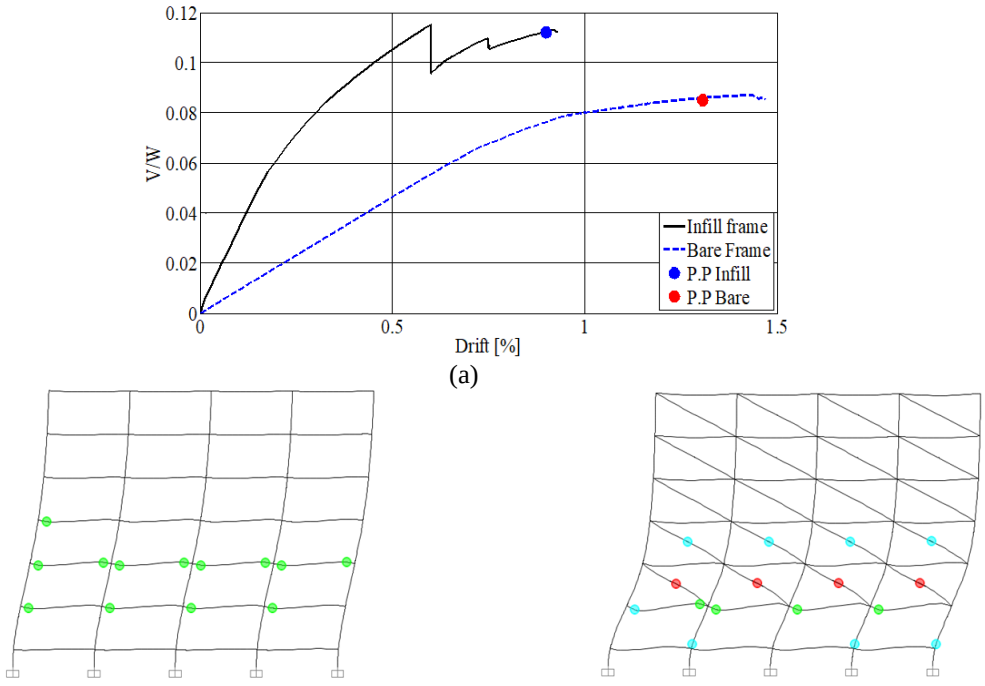

Figure 14 *(a) Capacity curve of bare and infill frames and damage pattern of structure at performance point of nonlinear static method (b) Bare frame and (c) Infilled frame.*

5.2 Effect of multiple excitations by considering infills in a structure

The response history analyses attempts to fully represent the seismic response of the structure without compromising the dynamic effects of the structure under a seismic event like its simplified counterparts i.e. linear static and nonlinear static procedures which tend to simplify the problem [Chambers and Kelly, 2004].

Non-linear dynamic response history is carried out using a suite of 7 single ground motions discussed in section 4.1 and 4.2 which are divided into 2 categories real and artificial seismic sequence to investigate the performance of reinforced concrete bare and infilled frames under multiple earthquakes loading. The response of frames is reported in terms of residual and transient inter-story drifts, residual and maximum floor displacements following the development of plastic hinges (damage pattern) in the structure.

5.2.1 Inter-story drift ratios

Inter-story drift ratio is the displacement normalized by story height of structure for particular level. Drift limits typically used for safeguarding against the loss of human life and property after a seismic event. According to ASCE 41-17 the drift limits are set for three performance levels i.e. Immediate Occupancy (IO), Life Safety (LS) and Collapse Prevention (CP) mentioned in Table 4. Although inter-story drift ratio do not account for effects of cumulative damage due to repeated inelastic deformation [Ghobarah *et al.*, 1999)]. The transient inter-story drift ratios are shown Figs. 15-21 and residual inter-story drift ratios are shown Figs. 22-28 for both bare and infill frames.

Deducing from the given plots, the ground motion sequences for majority of ground motions lead to larger drift values when compared with single ground motions. The transient inter-story drift ratio crosses the collapse limit state for the infill frames than that for their bare counterparts which indicates greater damage is induced in infilled frame. This behavior is repeated for residual inter-story drifts as well, and it can be seen that the bare frame remained well within the residual drift (Life safety) limit state while its infill counterpart crossed the threshold limit. Since the building being examined was a residential building the acceptance criteria was Life Safety performance level which exceeded in the case of infilled frame.

Table 4 *Inter-story drifts limits in ASCE codes*

Code	**Acceptance Criteria**	**Inter-Story Drift Limits**	
		Concrete Frame	**Unreinforced Masonry Infill Walls**
ASCE 41-17	**Immediate Occupancy**	1%	0.1%
	Life Safety	2% (transient) 1% (permanent)	0.5% (transient) 0.3% (permanent)
	Collapse Prevention	4 %	0.6%

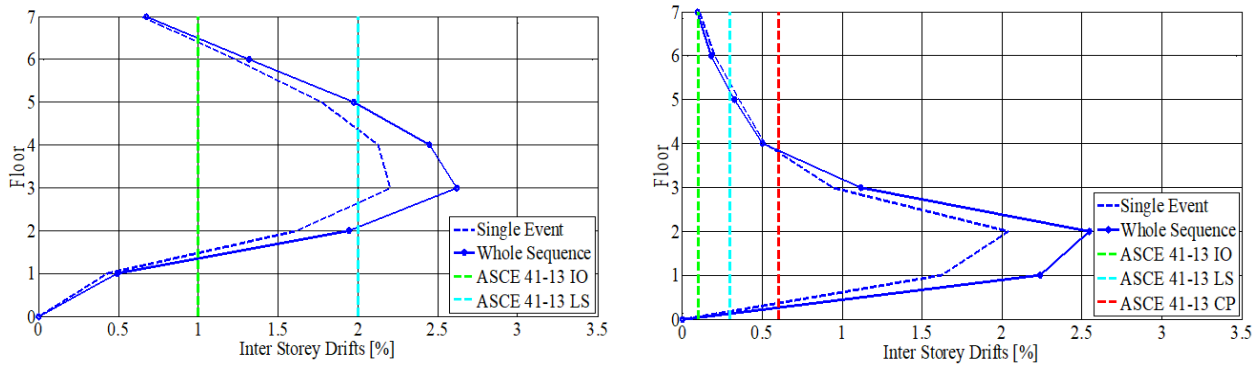

(a) (b)

Figure 15 *Transient inter-story drift ratio (%) profile under Altadena sequence for (a) Bare, and (b) Infill Frames.*

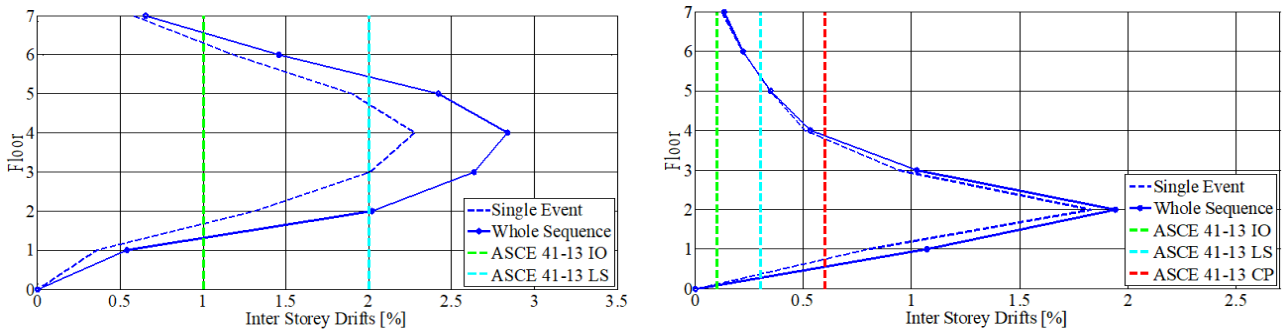

(a) (b)

Figure 16 *Transient inter-story drift ratio (%) profile under Corallit sequence for (a) Bare, and (b) Infill Frames.*

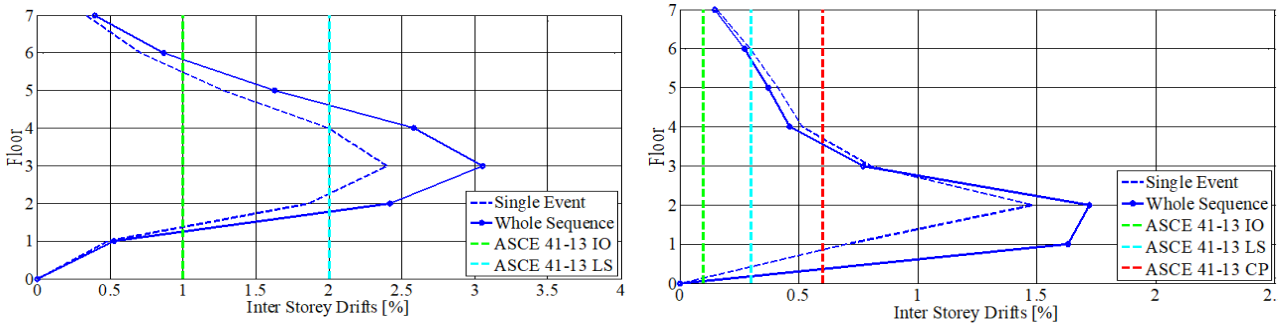

(a) (b)

Figure 17 *Transient inter-story drift ratio (%) profile under Santa Monica sequence for (a) Bare, and (b) Infill Frames.*

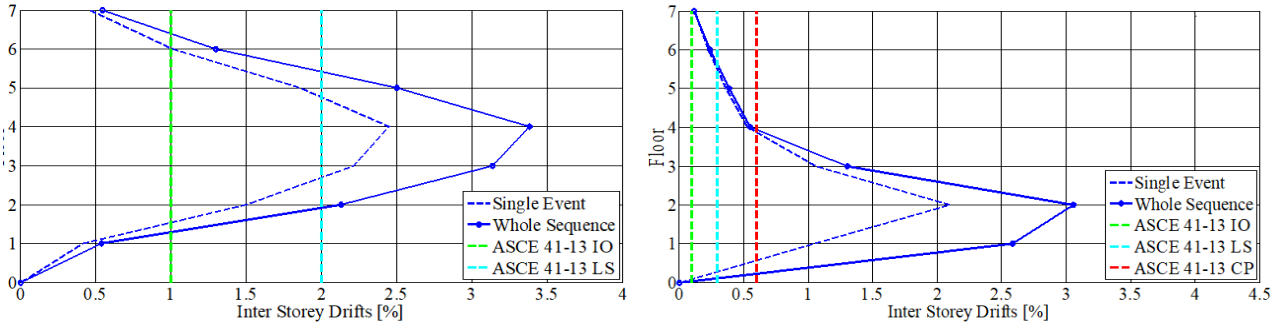

(a) (b)

Figure 18 *Transient inter-story drift ratio (%) profile under Hollister sequence for (a) Bare (b) Infill Frame.*

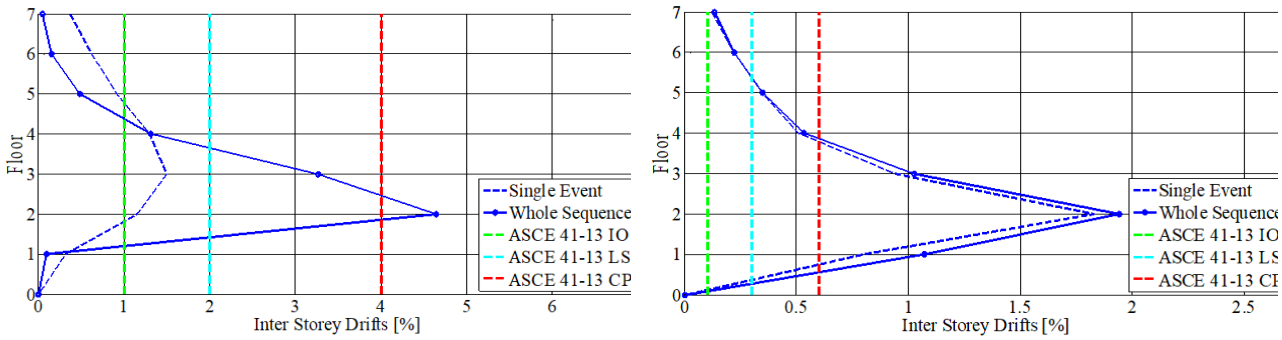

(a) (b)

Figure 19 *Transient inter-story drift ratio (%) profile under Coalinga sequence for (a) Bare, and (b) Infill Frames.*

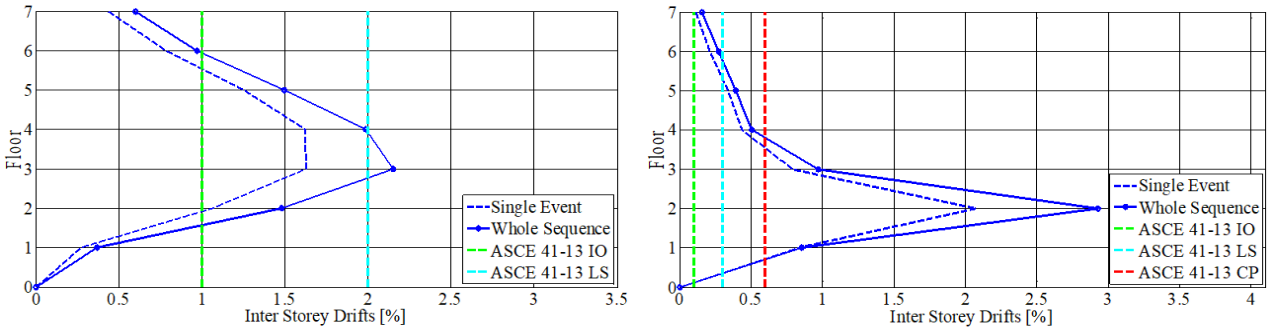

(a) (b)

Figure 20 *Transient inter-story drift ratio (%) profile under Whittier Narrows sequence for (a) Bare, and (b) Infill Frames.*

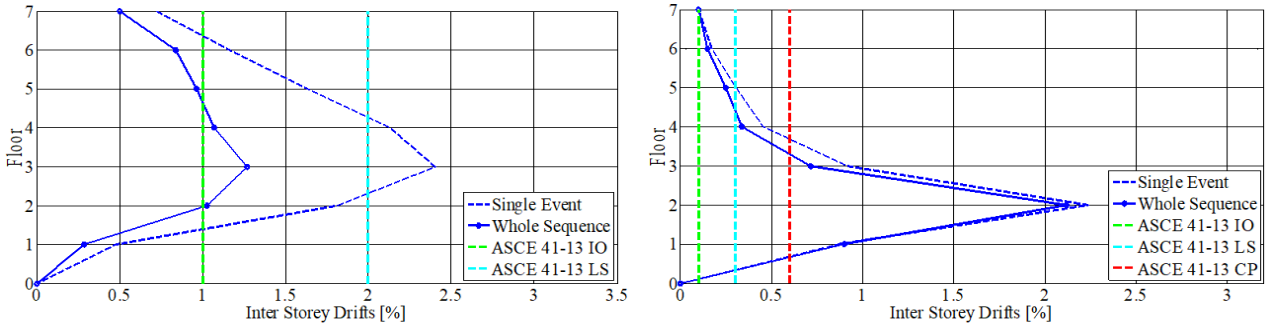

(a) (b)

Figure 21 *Transient inter-story drift ratio (%) profile under Imperial Valley sequence for (a) Bare, and (b) Infill Frames.*

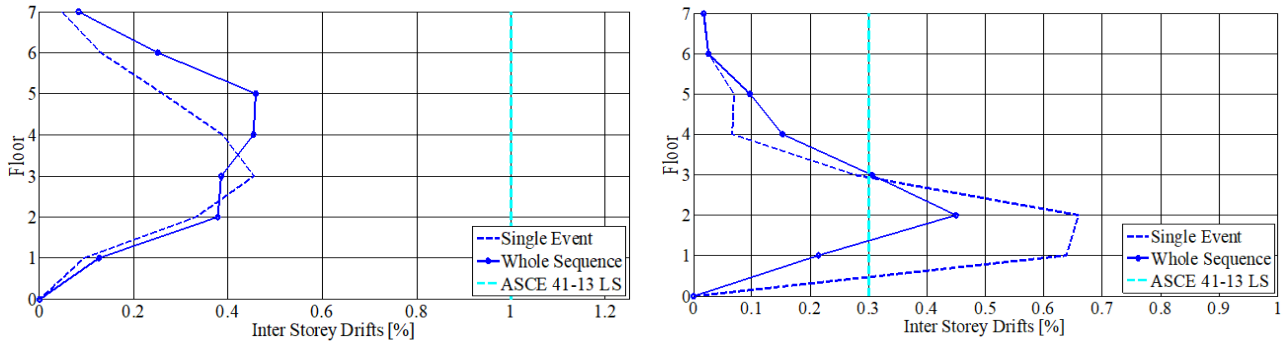

(a) (b)

Figure 22 *Residual inter-story drift ratio (%) profile under Altadena sequence for (a) Bare, and (b) Infill Frames.*

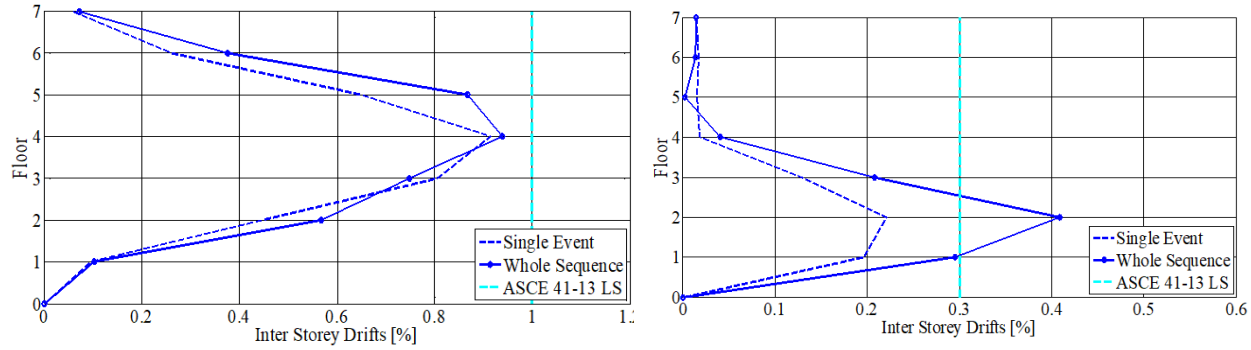

(a) (b)

Figure 23 *Residual inter-story drift ratio (%) profile under Corrallit sequence for (a) Bare, and (b) Infill Frames.*

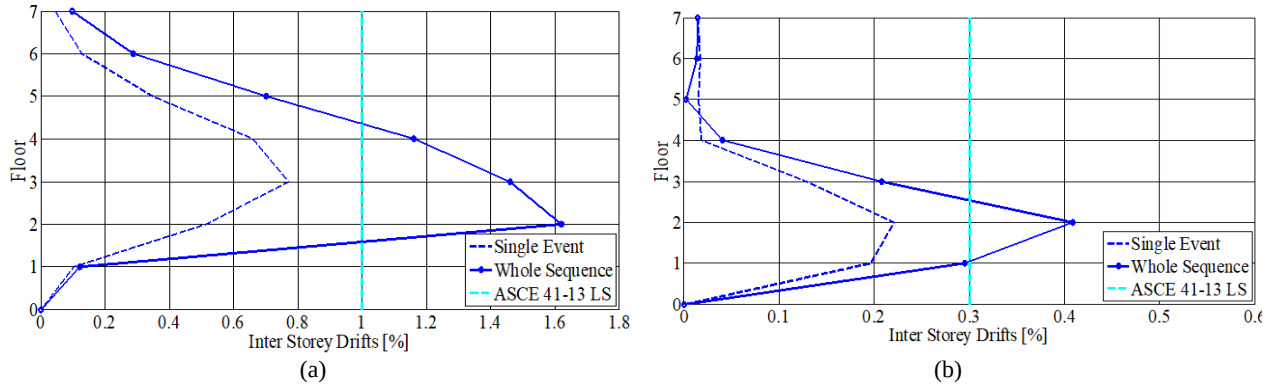

(a) (b)

Figure 24 *Residual inter-story drift ratio (%) profile under Santa Monica sequence for (a) Bare, and (b) Infill Frames.*

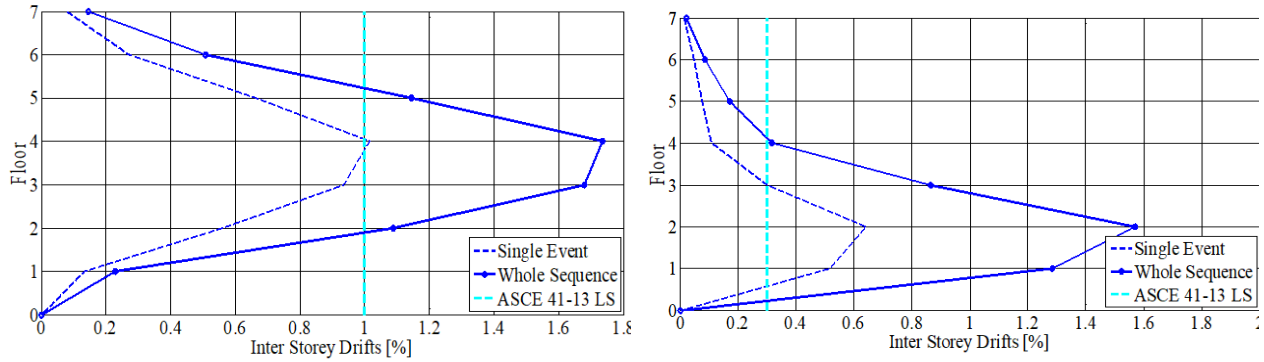

(a) (b)

Figure 25 *Residual inter-story drift ratio (%) profile under Hollister sequence for (a) Bare, and (b) Infill Frames.*

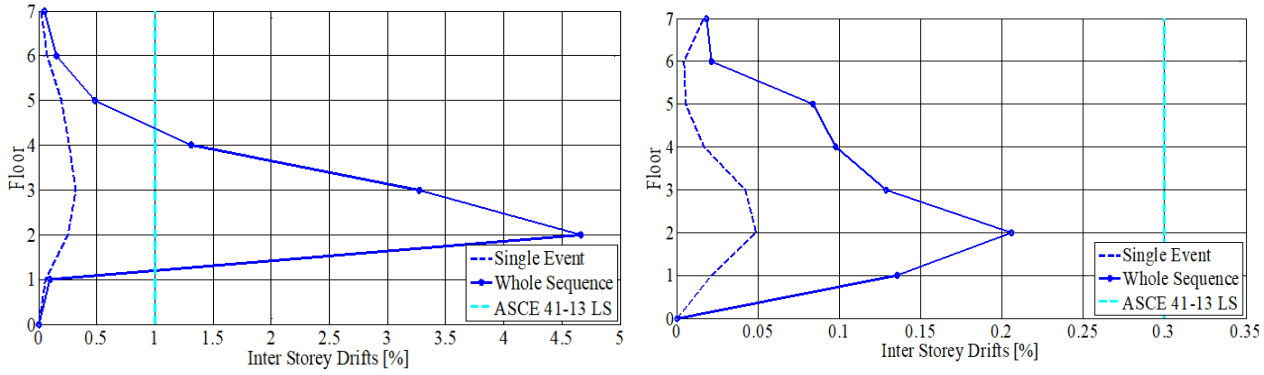

(a) (b)

Figure 26 *Residual inter-story drift ratio (%) profile under Coalinga sequence for (a) Bare, and (b) Infill Frames.*

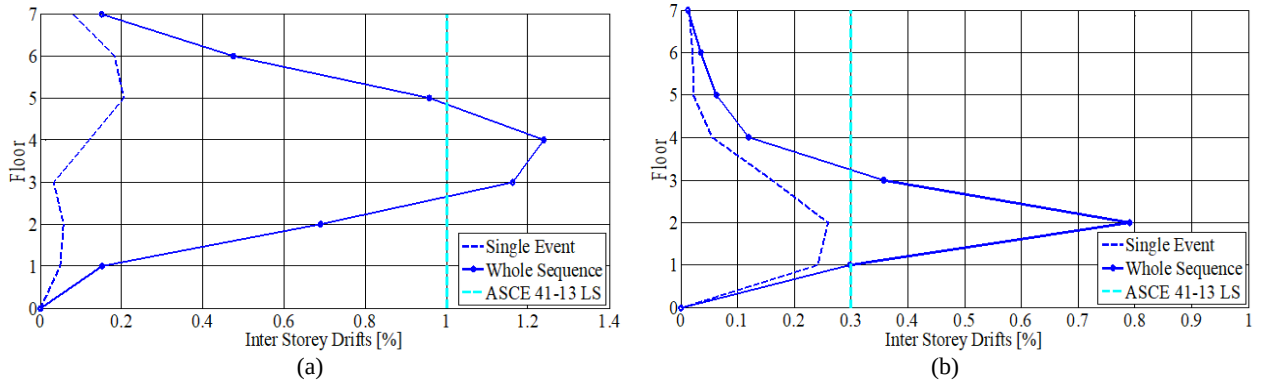

(a) (b)

Figure 27 *Residual inter-story drift ratio (%) profile under Whittier Narrows sequence for (a) Bare, and (b) Infill Frames.*

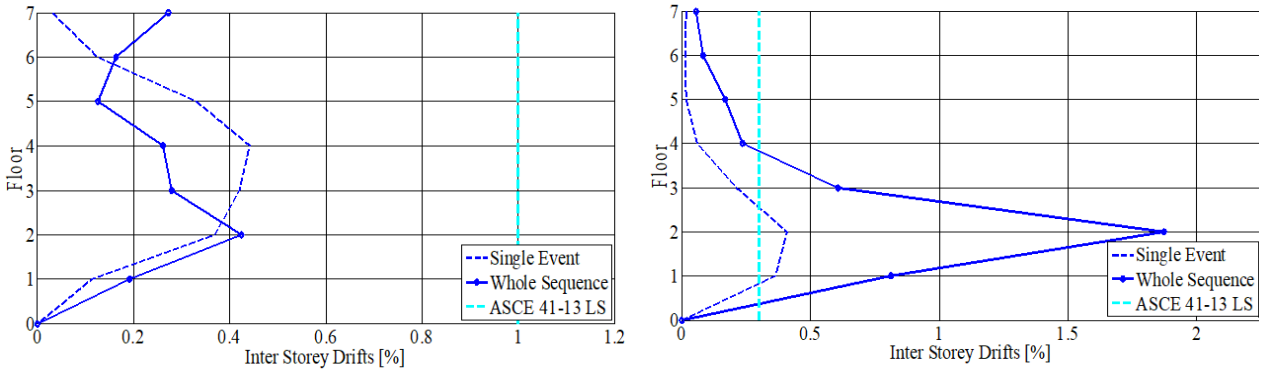

Figure 28 *Residual inter-story drift ratio (%) profile under Imperial Valley sequence for (a) Bare, and (b) Infill Frames.*

5.2.2 Maximum horizontal displacement

Results are also presented in the form of maximum horizontal displacement profiles for both real and artificial ground motions shown in Figs 29-35. In bare frame, results of single event shows good comparison with pushover results except for Whittier Narrows and Imperial Valley ground motions. However, in case of infilled frame, the pushover results over estimate displacement demand even as compared to the results obtained from ground motion sequences. It is concluded that significant increase in displacement demands for both the frames due to the multiplicity of earthquakes and since bare frame is more ductile it shows greater displacement demands when compared with infilled frame.

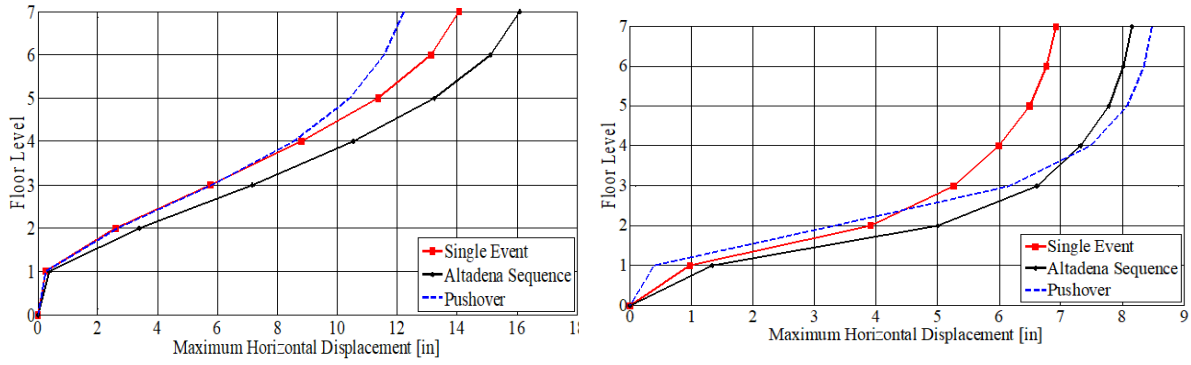

Figure 29 *Maximum horizontal displacement profile under Altadena sequence for (a) Bare, and (b) Infill Frames.*

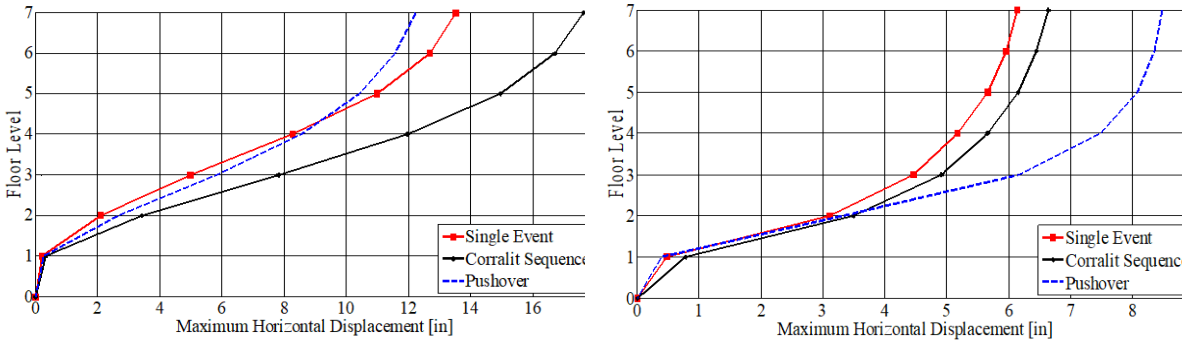

(a) (b)

Figure 30 *Maximum horizontal displacement profile under Corralit sequence for (a) Bare, and (b) Infill Frames.*

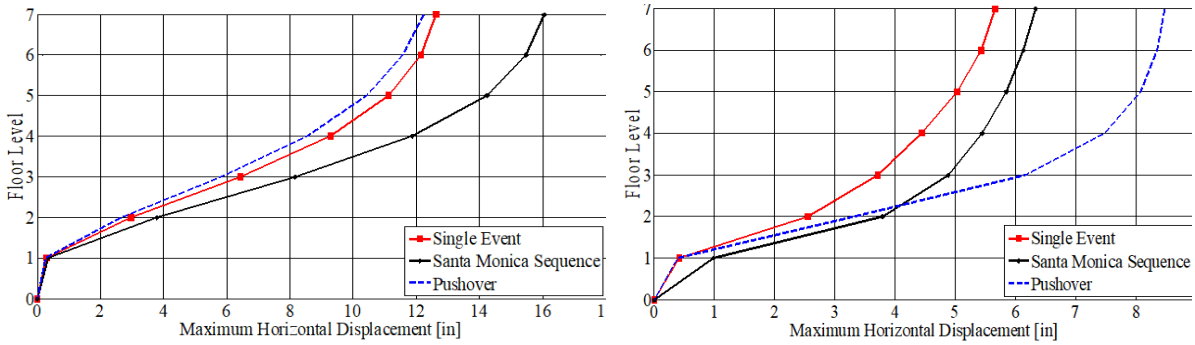

(a) (b)

Figure 31 *Maximum horizontal displacement profile under Santa Monica sequence for (a) Bare, and (b) Infill Frames.*

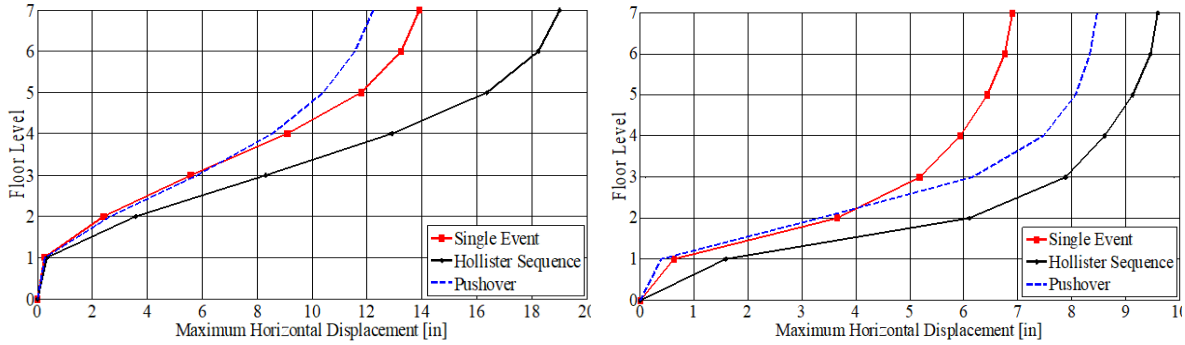

(a) (b)

Figure 32 *Maximum horizontal displacement profile under Hollister sequence for (a) Bare, and (b) Infill Frames.*

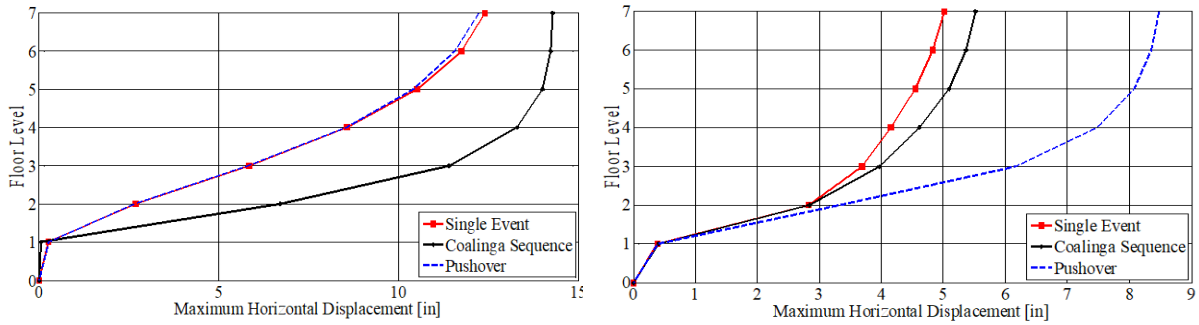

(a) (b)

Figure 33 *Maximum horizontal displacement profile under Coalinga sequence for (a) Bare, and (b) Infill Frames.*

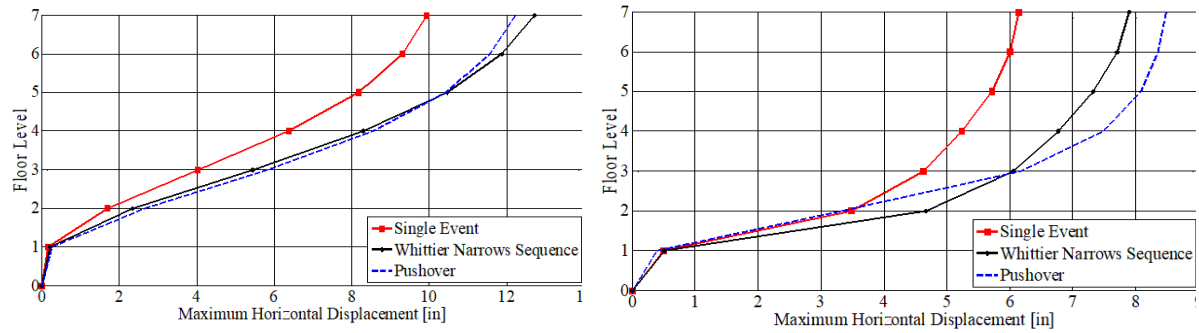

(a) (b)

Figure 34 *Maximum horizontal displacement profile under Whittier Narrows sequence for (a) Bare, and (b) Infill Frames.*

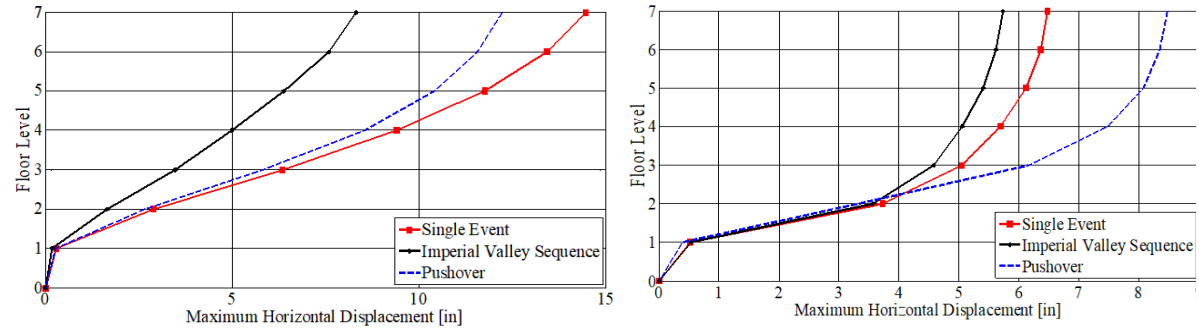

(a) (b)

Figure 35 *Maximum horizontal displacement profile under Imperial Valley sequence for (a) Bare, and (b) Infill Frames.*

5.2.3 Damage Patterns

The distribution of plastic hinges of bare and infilled frames, under the mentioned seismic sequences appears in Figs. 36-42 respectively. The damage pattern obtained after applying the ground motion record shows a progressive failure in both bare and infilled frames since the number of hinges increase in the second event for all the ground motions except for Imperial Valley since the structure collapsed in the first event to the point where it can no longer be damaged. Also the response of infilled frames is much severe when compared with their bare

counterparts since the columns above plinth level in infilled frames yielded during the first event of most earthquakes. Exceptional results were found only in Coalinga ground motion sequence where the bare frame collapsed under the second event as compared to infilled frame.

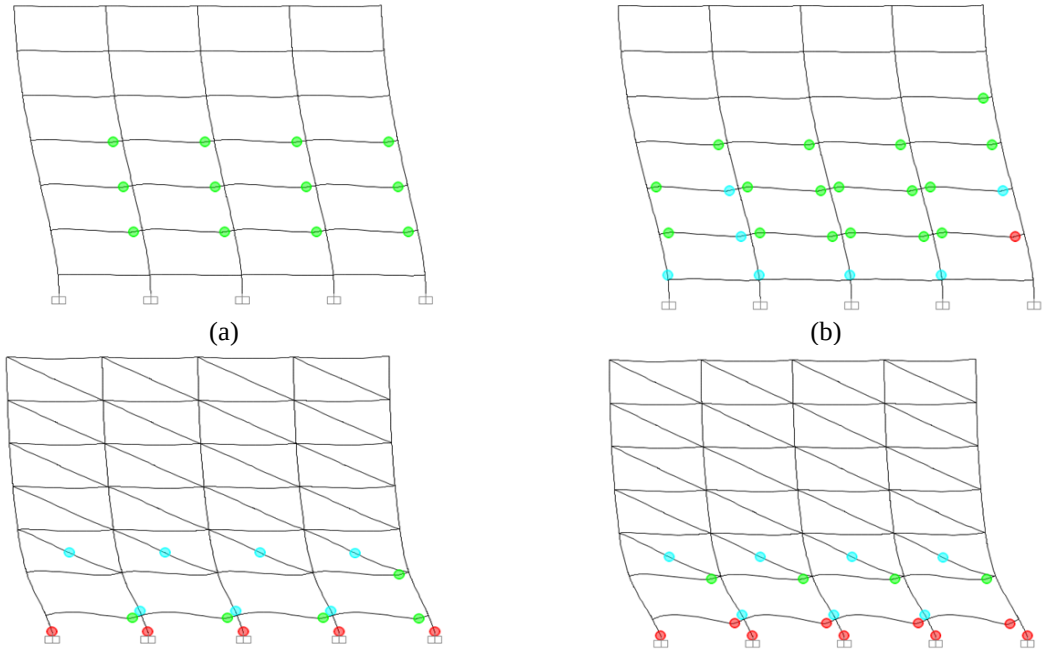

Figure 36 *Plastic hinge formation for Altadena ground motion (a) bare frame at event 1, (b) bare frame at event 2, (c) infill frame at event 1 and (d) infill frame at event 2.*

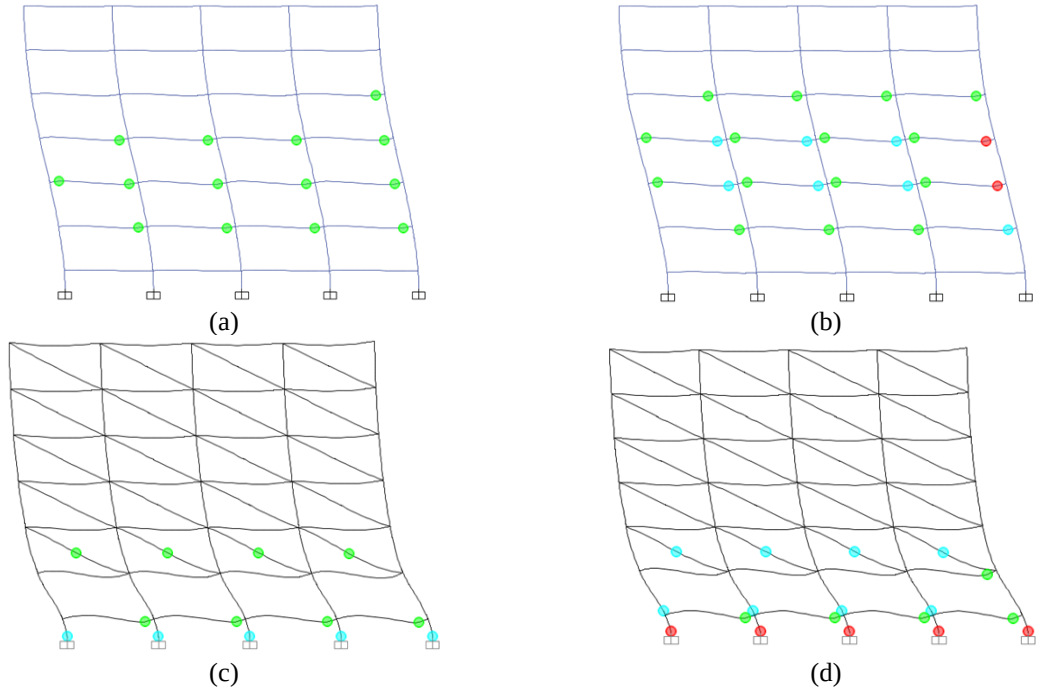

Figure 37 *Plastic hinge formation for Corralit ground motion (a) bare frame at event 1, (b) bare frame at event 2, (c) infill frame at event 1 and (d) infill frame at event 2.*

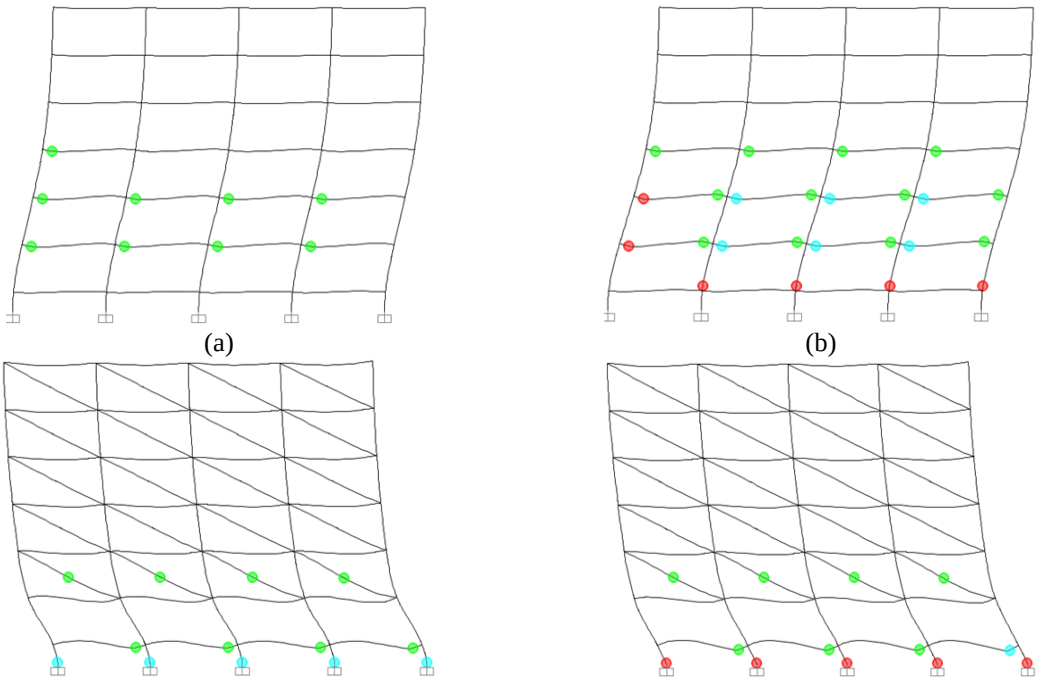

Figure 38 *Plastic hinge formation for Santa Monica ground motion (a) bare frame at event 1, (b) bare frame at event 2, (c) infill frame at event 1 and (d) infill frame at event 2.*

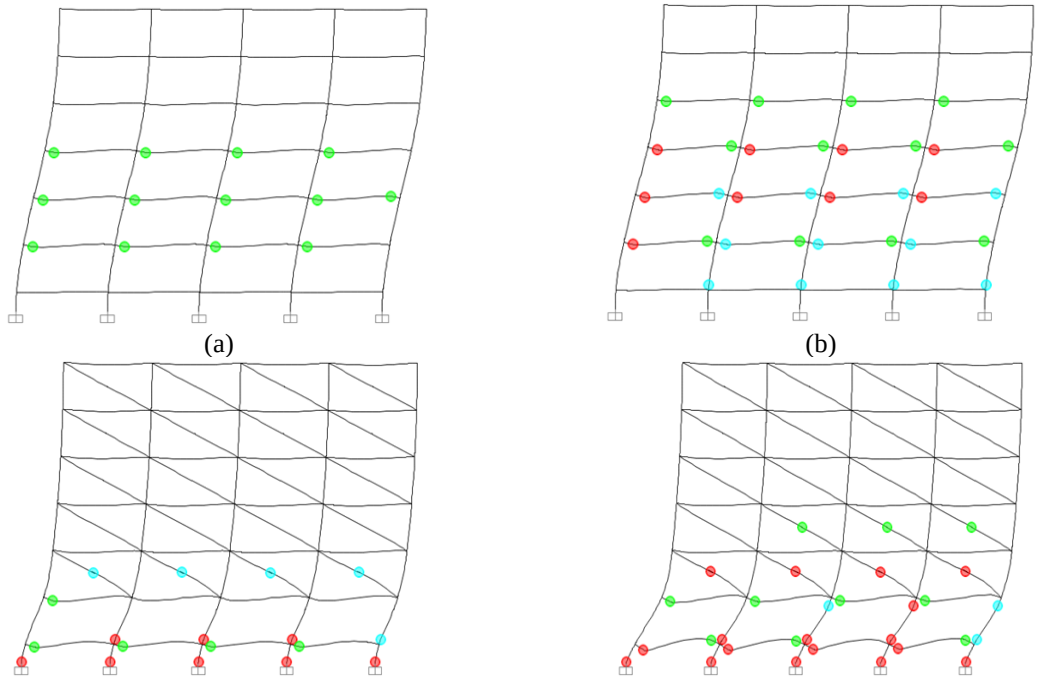

Figure 39 *Plastic hinge formation for Hollister ground motion (a) bare frame at event 1, (b) bare frame at event 2, (c) infill frame at event 1 and (d) infill frame at event 2.*

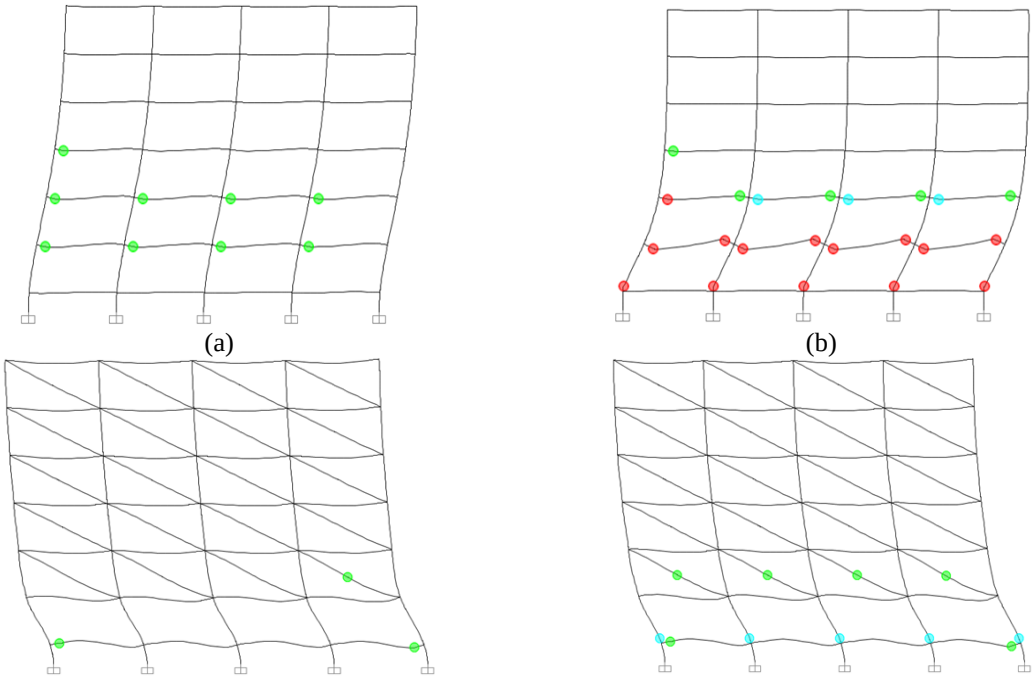

Figure 40 *Plastic hinge formation for Coalinga ground motion (a) bare frame at event 1, (b) bare frame at event 2, (c) infill frame at event 1 and (d) infill frame at event 2.*

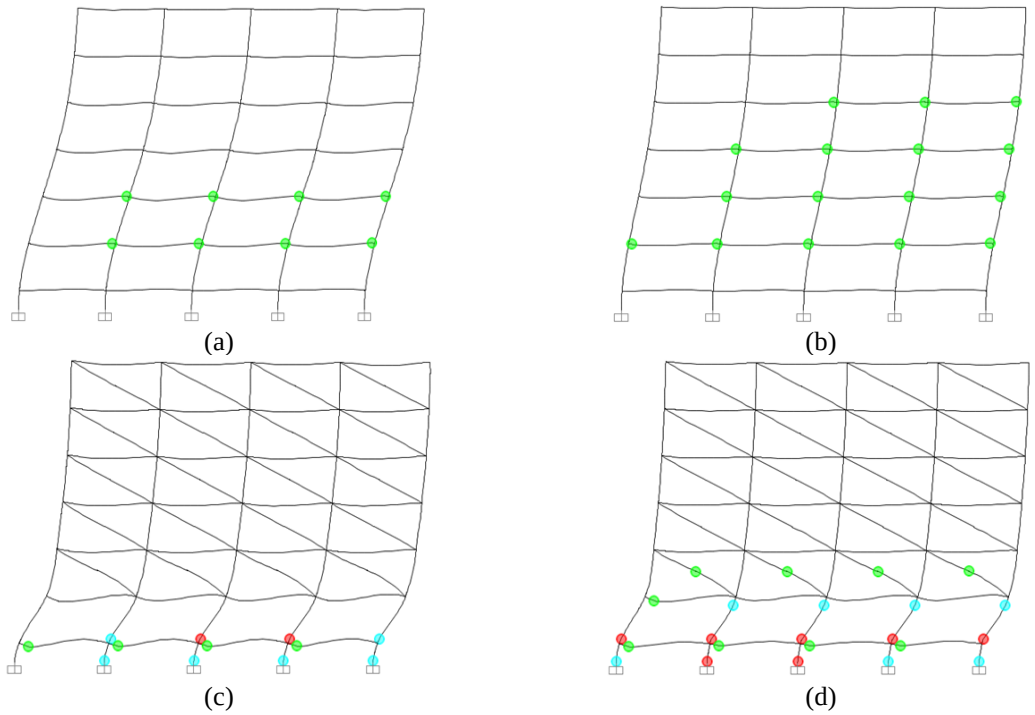

Figure 41 *Plastic hinge formation for Whittier Narrows ground motion (a) bare frame at event 1, (b) bare frame at event 2, (c) infill frame at event 1 and (d) infill frame at event 2.*

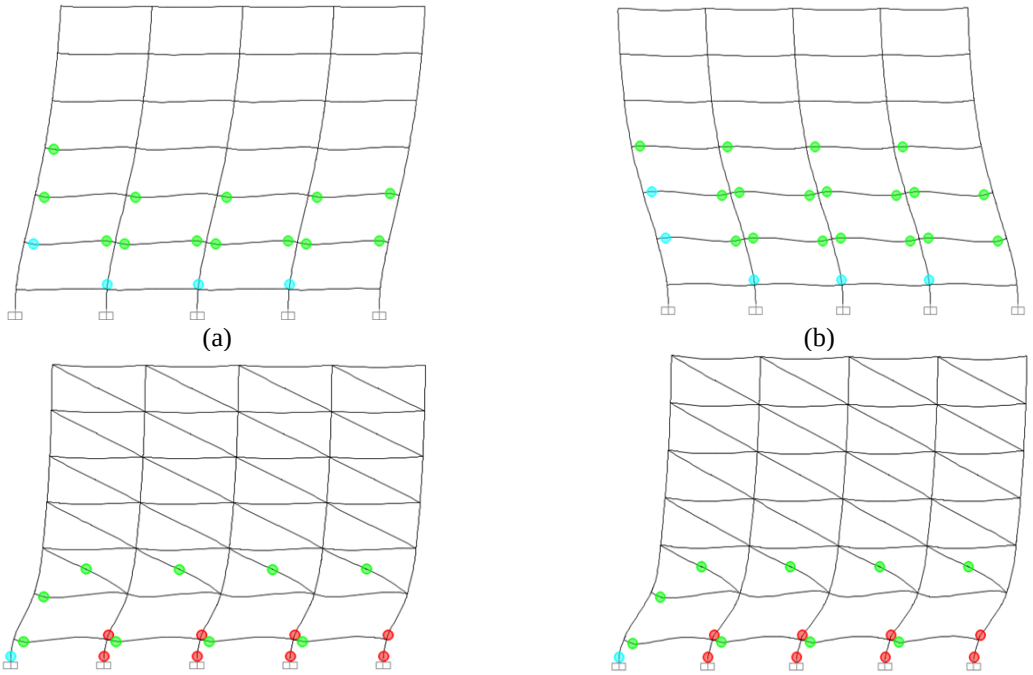

Figure 42 *Plastic hinge formation for Imperial Valley ground motion (a) bare frame at event 1, (b) bare frame at event 2, (c) infill frame at event 1 and (d) infill frame at event 2.*

5.2.4 Residual displacements

The residual displacements are strongly influenced by the array of earthquakes and it is inevitable to ignore the significance of multiple earthquake phenomena when estimating the displacements to meet the target performance levels. Figs. 43-49 show the roof displacement time traces of 7 ground motion sequences for bare and infilled frames. The seismic response from corresponding first and second event of all the ground motion sequences is illustrated on the plots to emphasize on the damage values. It can be concluded that the residual displacements in an infilled frame are much smaller than their bare counterparts but that does not specify the damage level since the threshold limit value of residual displacement for a bare frame is 1.44inches (36 mm) (equivalent to residual drift 1%) while for an infilled frame it's 0.43inches (11 mm) (equivalent to residual drift 0.3%). Almost in all ground motion sequences bare and infilled frames exceeding the residual drift limiting values.

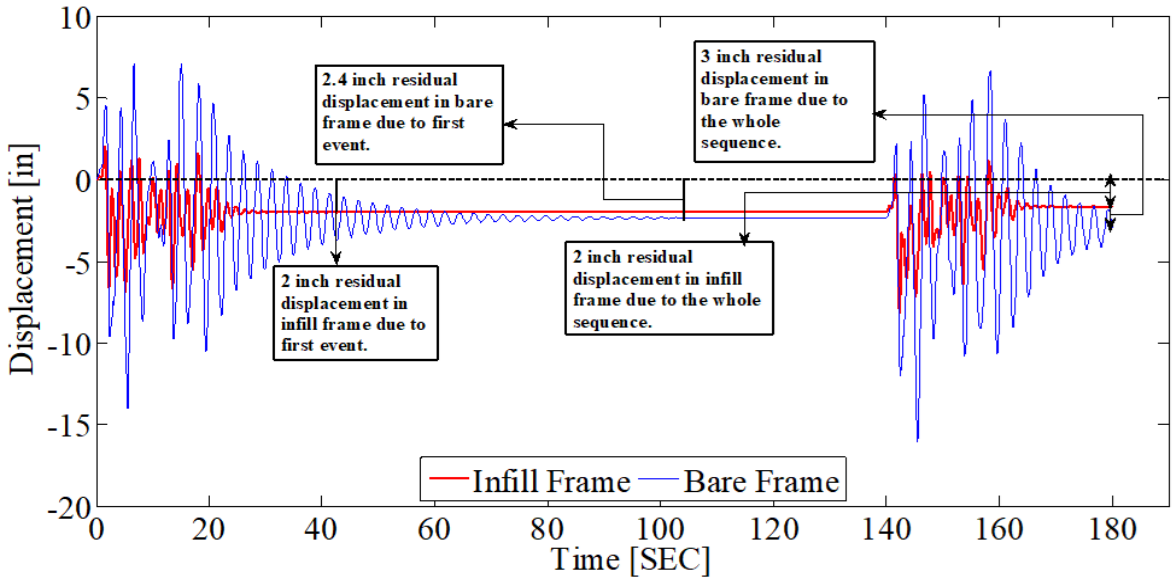

Figure 43 *Permanent displacement due to Altadena ground motion sequence for bare and infill frames.*

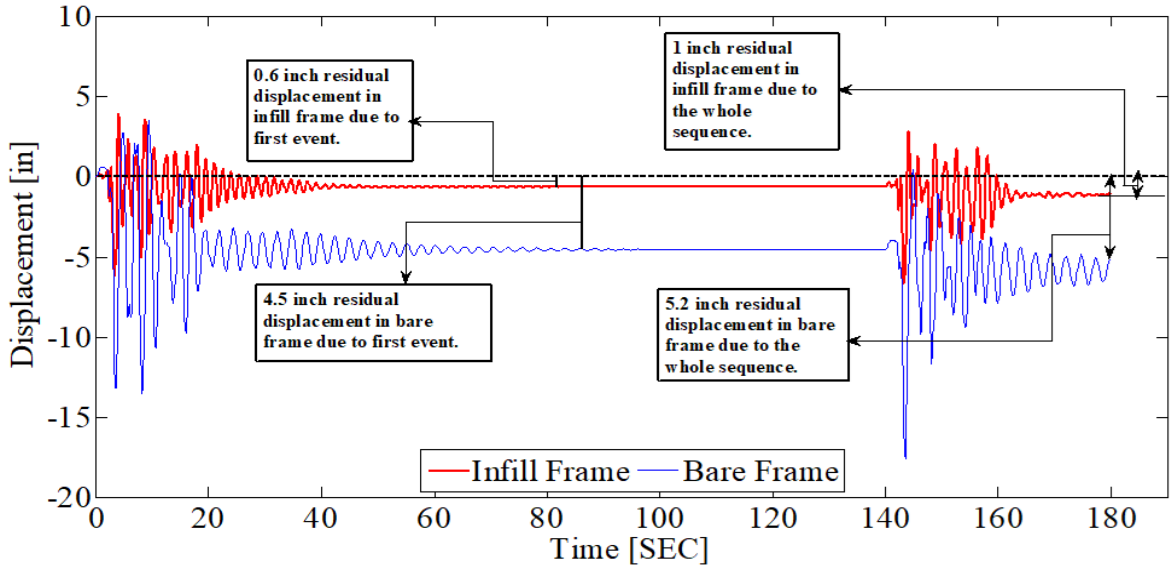

Figure 44 *Permanent displacement due to Corralit ground motion sequence for bare and infill frames.*

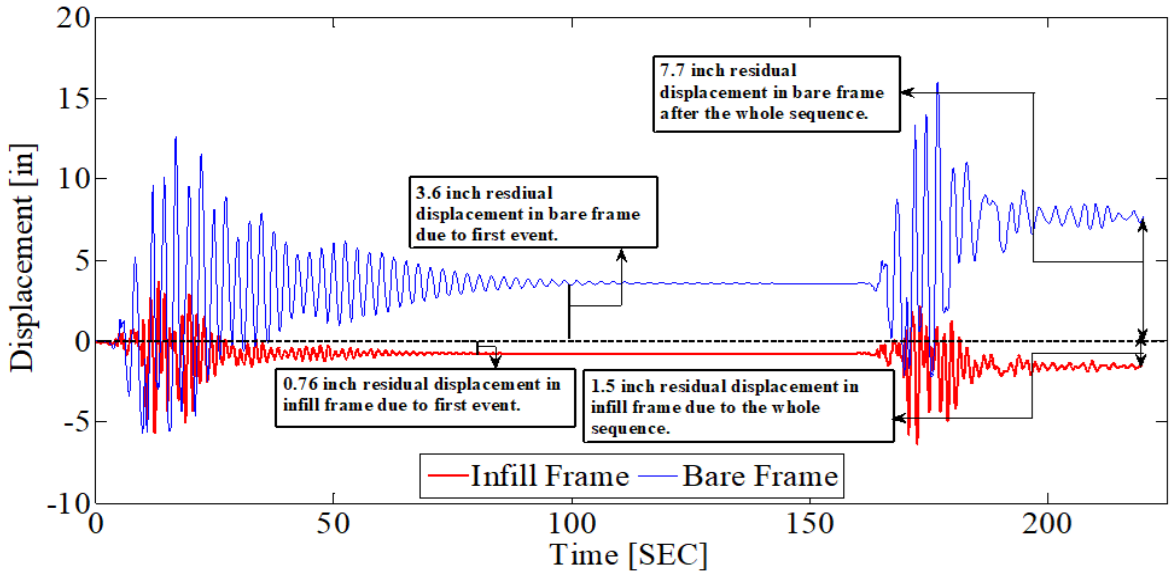

Figure 45 *Permanent displacement due to Santa Monica ground motion sequence for bare and infill frames.*

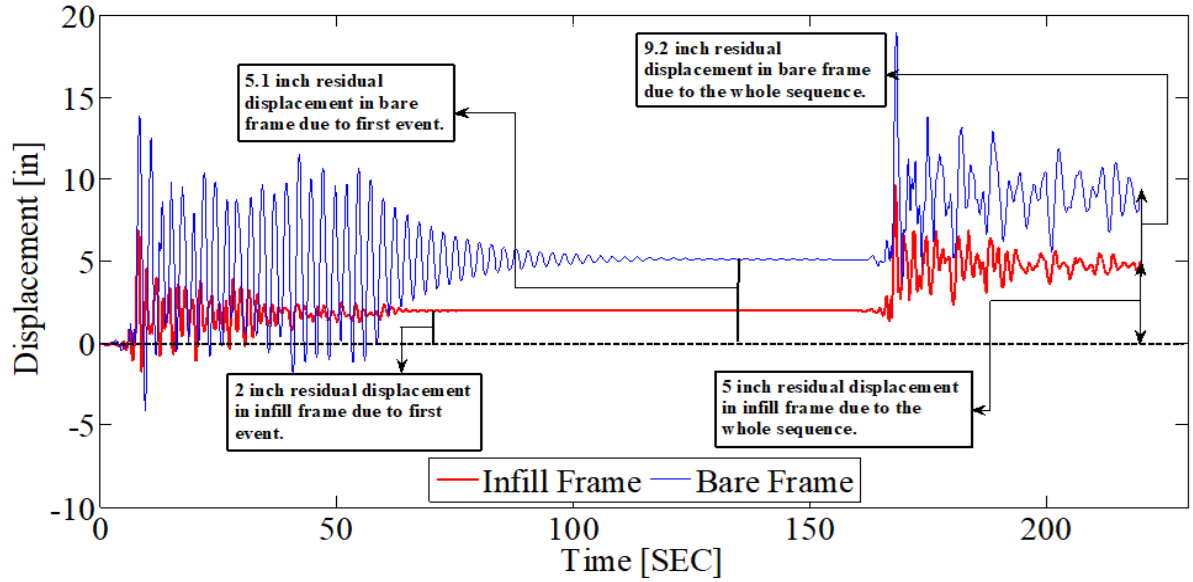

Figure 46 *Permanent displacement due to Hollister ground motion sequence for bare and infill frames.*

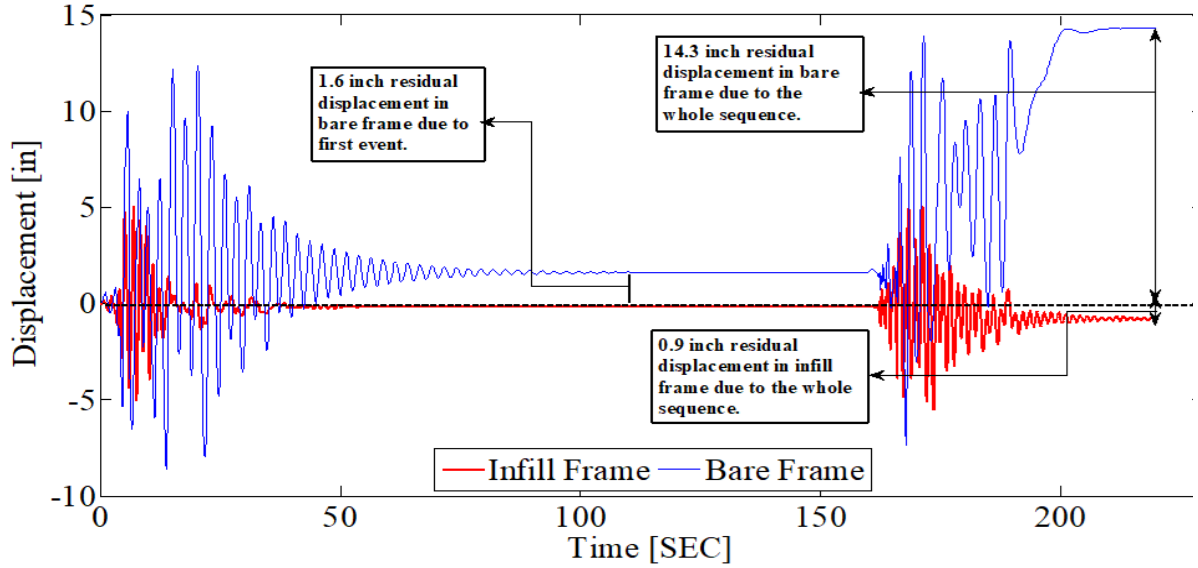

Figure 47 *Permanent displacement due to Coalinga ground motion sequence for bare and infill frames.*

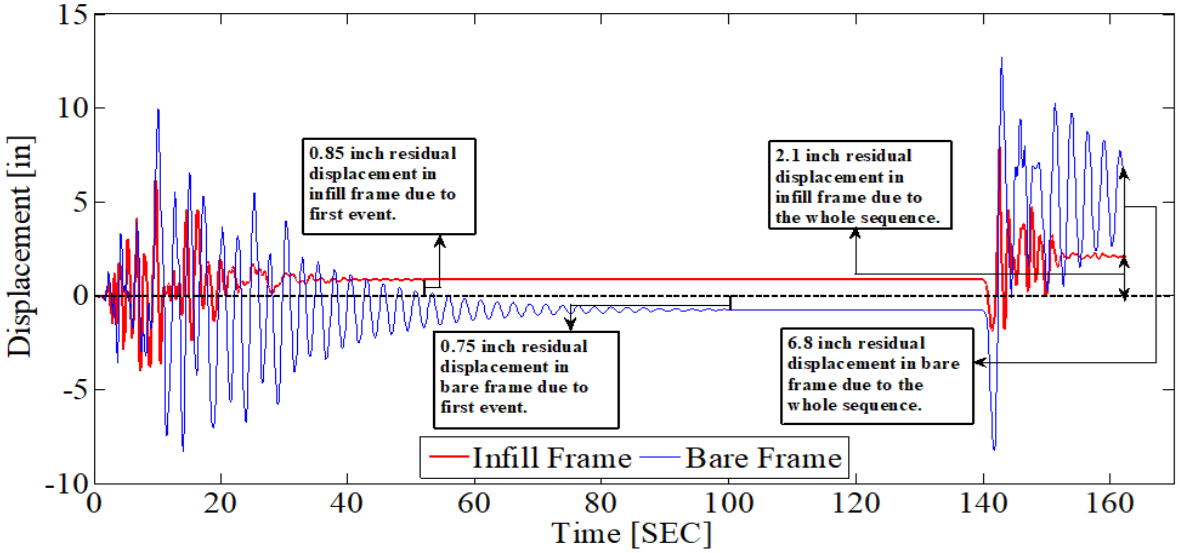

Figure 48 *Permanent displacement due to Whittier Narrows ground motion sequence for bare and infill frames.*

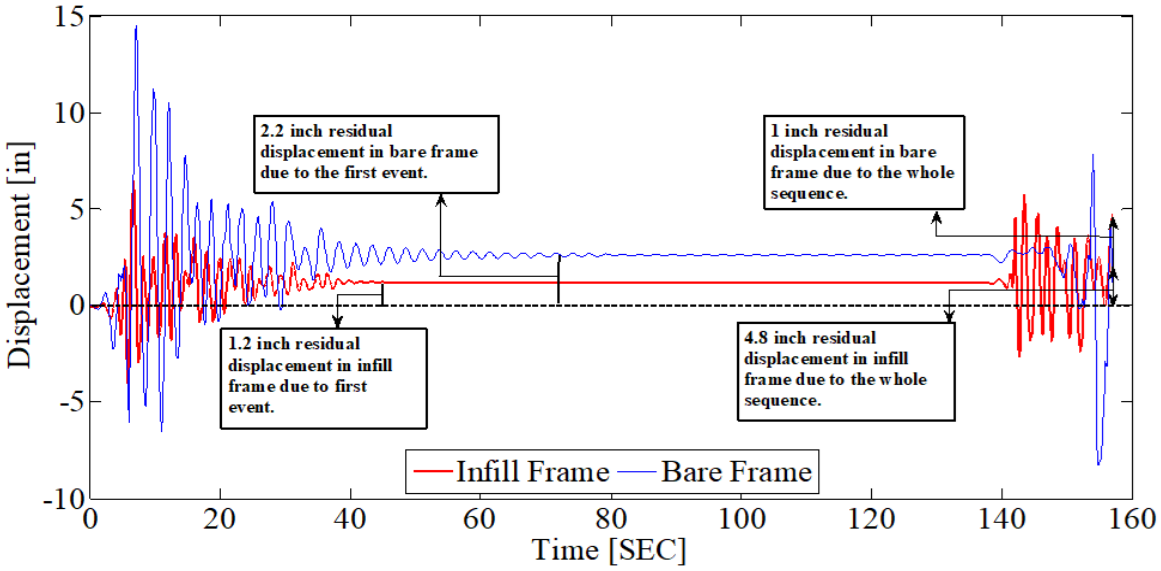

Figure 49 *Permanent displacement due to Imperial Valley ground motion sequence for bare and infill frames.*

6 Conclusions

Reinforced concrete structures are found to be most sensitive when exposed to the risk of multiple earthquakes. When a structure is subjected to multiple shocks it accumulates damage due to residual displacements which when exposed to the risk of aftershocks within a short interval of time affects its stiffness, strength and ductility.

In current study, a total of 7 earthquake sequences are applied to the reinforced concrete bare and infilled frames out of which three are real and four are synthetic repeated sequences. The response of the structure is measured in terms of inter-story drifts, maximum horizontal displacements, residual displacement and damage pattern for reinforced concrete bare and infilled frame systems leading to the following conclusions.

When a structure is subjected to multiple earthquakes it requires an increased demand of displacement as compared to the assessment based on main shock only. Earthquake sequence imposed higher displacement demands on infilled frame when compared with bare frame since the residual drifts limit according to ASCE 41-17 for an infill frame was 0.3% which was exceeded by 2.24% in Altadena, 1.07% in Corralit, 1.63% in Santa Monica, 2.58% in Hollister ,0.68% in Coalinga, 0.85% Whittier Narrows and 0.9% in Imperial Valley ground motion sequence.

The damage induced by earthquake sequence in an infilled frame is greater than that of a bare frame since all the ground motion sequences except for Coalinga sequence either formed weak stories or reached CP limit state while for bare frame, only Coalinga and Santa Monica sequences showed CP limit state on columns of story above plinth level.

The inter-story drift ratio's shows that infilled frames exceeded the CP limit state for all the ground motions since the code limit for CP was 0.6% for infilled which was exceeded by 1.62 % in Altadena, 0.8 % in Corralit, 0.7 % in Santa Monica, 1.05 % in Hollister, 0.64 % in Coalinga, 0.83 % Whittier Narrows and 0.87 % in Imperial Valley during the first event of sequence at the first story. While it's counter part of bare frame had a code limit of 1% for IO which was exceeded by 2.20 % in Altadena, 1.31 % in Corralit, 1.86 % in Santa Monica, 1.5 % in Hollister,

1.16 % in Coalinga, 1.06% Whittier Narrows and 2.40 % in Imperial Valley during the first event of sequence.

The inter-story drift ratio's shows that infill frames exceeded the CP limit state for all the ground motions in the first event which only progressed towards further failure of 2.54% in Altadena, 1.94% in Corralit, 1.72 % in Santa Monica, 3.06 % in Hollister, 1.7% in Coalinga, 2.93 % Whittier Narrows and 2.12 % in Imperial Valley during the second event of sequence. While it's counter part of bare frame had a code limit of 2% for LS limit state which was exceeded by 2.62 % in Altadena, 2.02 % in Corralit, 2.42 % in Santa Monica, 2.13 % in Hollister, 4.64 % in Coalinga. Two sequences which did not exceed the 2% limit are 1.48% Whittier Narrows and 1.03 % in Imperial Valley during the second event of sequence.

Inter-story drift ratios and formation of plastic hinge show that damage induced to frames in the first event was greater in infill frames when compared with its bare counterpart since the infill frames formed weak stories and reached to a collapse limit during the first event for most of the sequences. This accumulation of damage affected the performance of structure in the subsequent event attracting less seismic forces.

The comparison between infilled and bare frame shows that the infilled structure performed poorly and Collapsed under sequential ground motion while bare frames were within LS limit. Since the building was a residential building so it was examined for a performance level of Life Safety criteria which was fulfilled by considering a bare frame but was non-compliant when infill was considered.

It is evident from the results that the presence of infill created a shift in performance of the structure and performed poorly under the multiple ground motion sequence. Furthermore, in current study the presence of slab elements rigidity is not included in analyses which need to be incorporated in future research.

References

Abdelnaby, A. E. and Elnashai, A. S. (2012) 'Response of Degrading Reinforced Concrete Systems Subjected to Replicate Earthquake Ground Motions', *15th World Conference on Earthquake Engineering, Lisbon Portugal*, 1970.

Abdelnaby, A. E. and Elnashai, A. S. (2014) 'Performance of degrading reinforced concrete frame systems under the tohoku and christchurch earthquake sequences', *Journal of Earthquake Engineering*, 18(7), pp. 1009–1036. doi: 10.1080/13632469.2014.923796.

Ahmed, M., Lodi, S. H., and Rafi, M. M. (2019) 'Probabilistic Seismic Hazard Analysis Based Zoning Map of Pakistan Probabilistic Seismic Hazard Analysis Based Zoning Map of', 2469. doi: 10.1080/13632469.2019.1684401.

Amadio, C., Fragiacomo, M. and Rajgelj, S. (2003) 'The effects of repeated earthquake ground motions on the non-linear response of SDOF systems', *Earthquake Enginering and Structural Dynamics*, 32(2), pp. 291–308. doi: 10.1002/eqe.225.

Bentz E. C., and Collins M. P. (2000) 'RESPONSE-2000'. Available at: http://www.ecf.utoronto.ca/bentz/homeS.

Bertoldi, S. H., Decanini, L. D. and C. Gavarini (1993) 'Telai tamponati soggetti ad azioni sismiche, un modello semplificato: confronto sperimentale e numerico."', in *Atti del 6 Convegno Nazionale L'ingegneria sismica in Italia*.

Bilham, R., *Lodi, S. H., Hough, S., Bukhary, S., Khan, A.M., and Rafeeqi, S.F.A* (2007) 'Seismic hazard in Karachi, Pakistan: Uncertain past, uncertain future', *Seismological Research Letters*, 78(6), pp. 601–613. doi: 10.1785/gssrl.78.6.601.

Chambers, J. and Kelly, T. (2004) 'Nonlinear Dynamic Analysis - The Ony Option for Irregular Structures', *13th World Conference on Earthquake Engineering*, (1389), p. 9.

Chopra, A. K., and Goel, R. K. (2001) *A modal pushover analysis procedure to estimate seismic demands for buildings: Theory and preliminary evaluation., PEER Report 2001/03*.

Crisafulli, F. J. (1997) *Seismic behaviour of reinforced concrete structures with masonry infills, Civil Engineering*.

CSI (2016) 'CSI Analysis Reference Manual', *I: Berkeley (CA, USA): Computers and Structures INC*, p. 496. Available at: https://wiki.csiamerica.com/display/doc/CSI+Analysis+Reference+Manual.

El-Dakhakhni, W. W., Elgaaly, M., and Hamid, A. A. (2003) 'Three-strut model for concrete masonry-infilled steel frames', *Journal of Structural Engineering*, 129(2), pp. 177–185. doi: 10.1061/(ASCE)0733-9445(2003)129:2(177).
Fardis, M., and Panagiotakos T. B. (1997) 'Seismic Design and Response of Bare and Masonry infilled Reinforced Concrete Buildings. Part Ii: Infilled Structures', *Journal of Earthquake Engineering*.

FEMA356 (2000) 'Prestandard and Commentary for the Seismic Rehabilitation of Buildings', *Rehabilitation Requirements*, (1), pp. 1–518.

Ghobarah, A., Abou-Elfath, H., and Biddah, A. (1999) 'Response-based damage assessment of structures', *Earthquake Engineering and Structural Dynamics*, 28(1), pp. 79–104. doi: 10.1002/(SICI)1096-9845(199901)28:1<79::AID-EQE805>3.0.CO;2-J.

Gomes, A. and Appleton, J. (1997) 'Nonlinear cyclic stress-strain relationship of reinforcing bars including buckling', *Engineering Structures*, 19(10), pp. 822–826. doi: 10.1016/S0141-0296(97)00166-1.

Hanson, R. D. (1996) 'Evaluation of reinforced concrete members damaged by earthquakes', *Earthquake Spectra*. Earthquake Engineering Research Institute, 12(3), pp. 457–478. doi: 10.1193/1.1585893.

Hatzigeorgiou, G. D. (2010) 'Ductility demand spectra for multiple near- and far-fault earthquakes', *Soil Dynamics and Earthquake Engineering*. Elsevier, 30(4), pp. 170–183. doi: 10.1016/j.soildyn.2009.10.003.

Hatzigeorgiou, G. D., and Beskos, D. E. (2009) 'Inelastic displacement ratios for SDOF structures subjected to repeated earthquakes', *Engineering Structures*. Elsevier Ltd, 31(11), pp. 2744–2755. doi: 10.1016/j.engstruct.2009.07.002.

Hatzigeorgiou, G. D., and Liolios, A. A. (2010) 'Nonlinear behaviour of RC frames under repeated strong ground motions', *Soil Dynamics and Earthquake Engineering*. Elsevier, 30(10), pp. 1010–1025. doi: 10.1016/j.soildyn.2010.04.013.

Lee, J., and Fenves, G. L. (1998) 'Plastic-damage model for cyclic loading of concrete structures', *Journal of Engineering Mechanics*, 124(8), pp. 892–900. doi: 10.1061/(ASCE)0733-9399(1998)124:8(892).

Lee, J. H., and Fenves, G. L. (1998) 'Plastic-damage model for cyclic loading of concrete structures', *J. Eng. Mech. (ASCE)*, 124(8), pp. 892–900.

Li, Q., and Ellingwood, B. R. (2007) 'Performance evaluation and damage assessment of steel frame buildings under mainshock-aftershock sequences.', *Earthquake Engineering and Structural Dynamics*, 3(36), pp. 405–427.

Mahin, S. A. (1980) 'Effects of Duration and Aftershocks on Inelastic Design Earthquakes.', in. Turk Natl Comm on Earthquake Eng, Ankara, pp. 677–680.

MAINSTONE R.J. (1971) 'On the stiffnesses and strengths of infilled frames', *Proc Inst Civ Eng, Suppl (iv)*, pp. 57–90.

MoHW (2007) *Building code of Pakistan (Seismic Provisions-2007).* Islamabad: Islamabad: Ministry of Housing & Works (MOHW) Government of Pakistan (GoP).

Mosalam, K. M., Park, S., and Günay, M. S. (2009) 'Evaluation of an Element Removal Algorithm for Reinforced Concrete Structures Using Shake Table Experiments', in *Proceedings of the 2nd International Conference on Computational Methods in structural Dynamics and Earthquake Engineering*. Island of Rhodes, Greece.

Montuori R, Nastri E, and Piluso V. (2016) Modelling of floor joists contribution to the lateral stiffness of RC buildings designed for gravity loads. Eng Struct;121:85–96.

Montuori R, Nastri E, Palese, M., and Piluso V. (2019). The effect of floor joists on the elastic and inelastic behavior of RC frames. Eng Struct; 196.http://dx.doi.org/10.1016/j.engstruct.2019.06.03.

Montuori R, Nastri E., Piluso V., and Streppone, S. (2021). Experimental validation of a theoretical model accoundting for floor joists contribution on the flexural resistance of beam-column joints in RC frames. Eng Struct; 247.http://doi.org/10.1016/j.engstruct.2021.113168.

Mwafy, A. M., and Elnashai, A. S. (2014) ‘Static pushover versus dynamic collapse analysis of RC buildings.’, *Journal of Engineering Structures*, 23, pp. 407–424. doi: https://doi.org/10.1016/S0141-0296(00)00068-7.

NED and GHI (2012) *6-Storey Mixed Use Building in Karachi: A pilot Case Study of Seismic Assessment and Retrofit Design*.

Oyguc, R., Toros, C., and Abdelnaby, A. E. (2018) ‘Seismic behavior of irregular reinforced-concrete structures under multiple earthquake excitations’, *Soil Dynamics and Earthquake Engineering*. Elsevier Ltd, 104(October 2017), pp. 15–32. doi: 10.1016/j.soildyn.2017.10.002.

Pacific Earthquake Engineering Research Center. (2017) *PEER*.

Ruiz-García, J. (2012) ‘Mainshock-aftershock ground motion features and their influence in building’s seismic response’, *Journal of Earthquake Engineering*, 16(5), pp. 719–737. doi: 10.1080/13632469.2012.663154.

UBC-1997 (1997) *Uniform building code, American Association of Building Officials, Whittier, CA*.

Waseem, M., Khan, M. A., and Khan, S. (2019) ‘Seismic sources for southern Pakistan and seismic hazard assessment of Karachi’, *Natural Hazards*. Springer Netherlands, 99(1), pp. 511–536. doi: 10.1007/s11069-019-03755-5.

ingegneria sismica
International Journal of Earthquake Engineering
Anno XXXVIII – Num.4 - 2021

VALUTAZIONE DELLA VULNERABILITÀ SISMICA DI EDIFICI ESISTENTI IN C.A. SOGGETTI A SEQUENZE SISMICHE

Kainaat Nadeem[1], *Aslam Faqeer Mohammad*[2]

[1, 2] Department of Civil Engineering, NED University of Engineering and Technology, Karachi, Pakistan

SOMMARIO: *Diversi terremoti si verificano in tutto il mondo dove esistono complessi sistemi di faglie. Una struttura danneggiata da un terremoto è esposta al rischio di scosse di assestamento entro un breve intervallo di tempo, che accumulano danni alla struttura e che influiscono sulla sua rigidezza, resistenza e duttilità. Questo studio si propone di indagare la risposta di telai in cemento armato con tamponature soggetti a sequenze sismiche. Un modello computazionale bidimensionale di un edificio in c.a. esistente situato a Karachi, in Pakistan, è prima analizzato come telaio nudo e poi con l'inserimento di tamponature. Inizialmente, l'analisi pushover è stata utilizzata per stimare la capacità e i modelli di danno dei telai. Infine, per tracciare la risposta completa, i frame selezionati sono stati sottoposti a tre sequenze sismiche reali (registrate a un breve intervallo di tempo presso la stessa stazione con la stessa direzione) e quattro sequenze sismiche ripetute generate artificialmente. I risultati sono presentati sotto forma di Engineering Demand Parameters (EDP), che conforma gli effetti di più terremoti, in particolare nel caso di telaio con tamponature.*

KEYWORDS: *Multiple Earthquakes, Nonlinear Pushover Analysis, Response History Analysis, Infilled frame, Residual Displacement, Residual Drift*

Corresponding author: Kainaat Nadeem, Department of Civil Engineering, NED University of Engineering and Technology, Pakistan.
Email: kainaat@neduet.edu.pk